

FACTS-Compensated Transmission System

5.1 INTRODUCTION

The stability and economy of a power system largely depends upon reliability and efficiency of the transmission networks, which can be improved by high speed distance protection schemes. However, these protection schemes are influenced by the compensated devices which are used for enhancement of power transfer capability and the power quality. Such devices include SSSC, STATCOM, UPFC, SVC, etc. These devices have versatile performance and complex structure. The presence of compensating device in a fault loop affects signals at the relay point, which may lead to over-reach or under-reach, in case of conventional distance protection. This is due to change in apparent impedance, affected by voltage and current signals injected by FACTS devices. Hence there is a need to explore the capability of signal processing techniques and artificial intelligence techniques which can overcome the limitations of conventional distance protection scheme.

5.2 PROPOSED ALGORITHM

The voltage and current signals, measured at both the buses are sampled with a frequency of 1920 Hz. This sampling is synchronized by GPS clock. The current signals, obtained over a moving window of quarter cycle, are analyzed with wavelet transform. The alienation coefficients are calculated by comparing the approximate coefficients of current window (W_0) with those of previous window (W_{-1}), at local buses, as illustrated in Figure 5.1. Fault Index is computed as summation of alienation coefficients obtained from local and remote buses. The proposed algorithm is enabled only when bus currents have a direction away from the buses.

Under normal operating conditions, the alienation coefficients obtained from windows W_0 and W_{-1} , would remain at zero value (and hence the fault index) due to their identity. However, in case of a disturbance, the alienation coefficients would attain a finite value (and hence the fault index), due to the dissimilarities in the signals. This fault index is compared with a threshold value ($F\text{-TH} = 0.2$) to detect the fault. The flow chart for the proposed algorithm is illustrated in Figure 5.1.

5.3 STATCOM-COMPENSATED TRANSMISSION SYSTEM

5.3.1 System Model and Parameters

The block diagram of the system, under consideration, is illustrated in Figure 5.2. The system parameters are presented in Table 5.1 [Dash, Das and Moirangthem, 2015]. The STATCOM is installed at the middle of the transmission line, rated 500kV, 60 Hz.

Table 5.1: System Parameters

AC Source	
For Bus-1 and Bus-2 Source	$Z=2.9142+j29.4117 \Omega$
Transmission Line Parameters (230 km)	
Resistance	$R_1=0.0250 \Omega/\text{km}, R_0=0.3864 \Omega/\text{km}$
Inductance	$L_1=9.3370 \times 10^{-4} \text{ H}/\text{km}, L_0=4.1264 \times 10^{-3} \text{ H}/\text{km}$
Capacitance	$C_1=12.74 \times 10^{-8} \text{ F}/\text{km}, C_0=7.751 \times 10^{-9} \text{ F}/\text{km}$
STATCOM	
48-pulse IGBT-based converter with 15/500 kV zigzag transformers rated at 100 MVA	

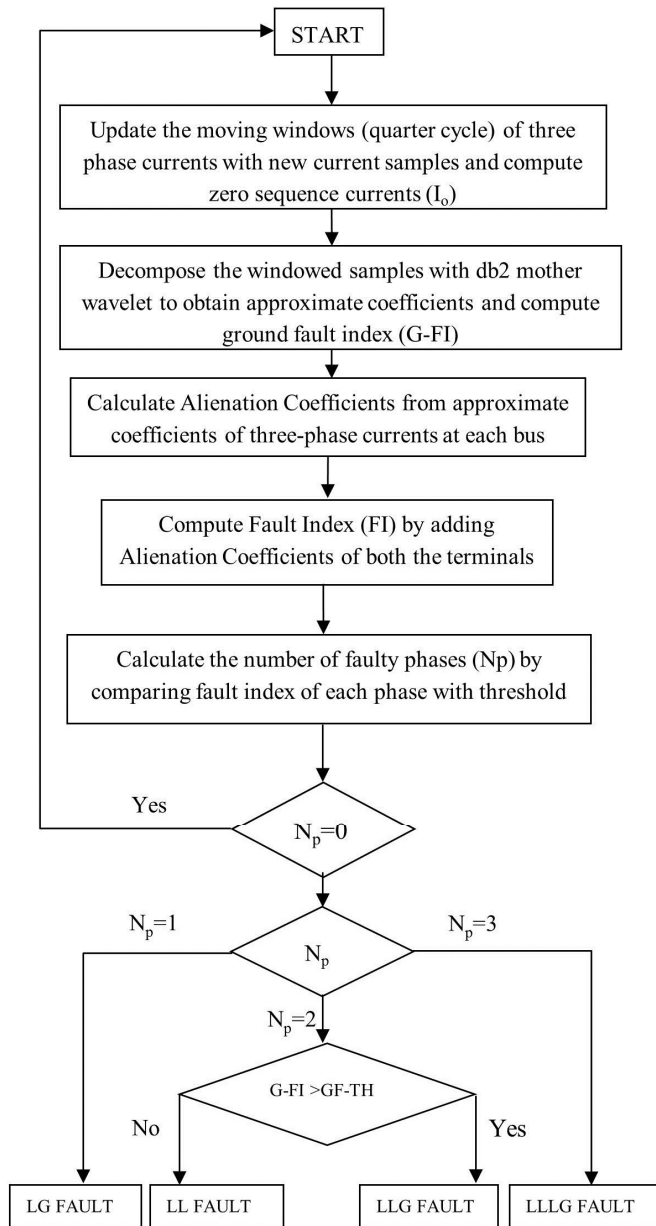


Figure 5.1: Flow chart of proposed scheme

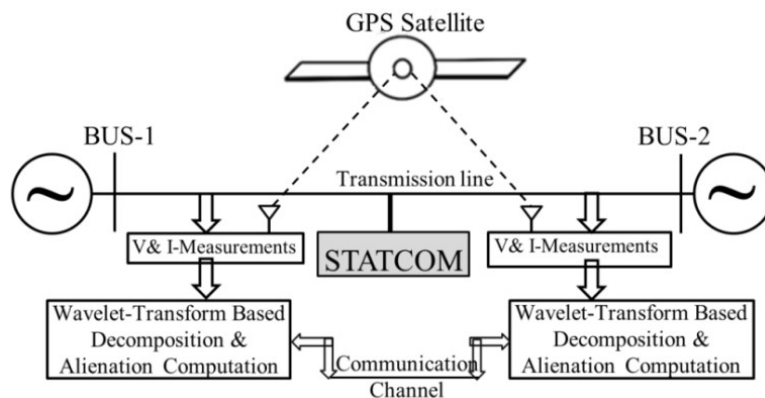


Figure 5.2: STATCOM-Compensated Transmission System

5.3.2 Fault Detection and Classification

Figure 5.3 demonstrates, various steps involved in detection of AG fault. Figures 5.3(a) and 5.3(b) show three-phase current signals measured at bus-1 and bus-2. The respective approximate coefficients are plotted in Figures 5.3(c) and 5.3(d). The alienation coefficients, obtained over a quarter cycle, based on these approximate coefficients are plotted in Figures 5.3(e) and 5.3(f). Figure 5.3(g) illustrates variation of fault index, computed by adding alienation coefficients of both the buses. It can also be observed that fault index of phase-A alone exceeds the threshold value, indicating AG fault.

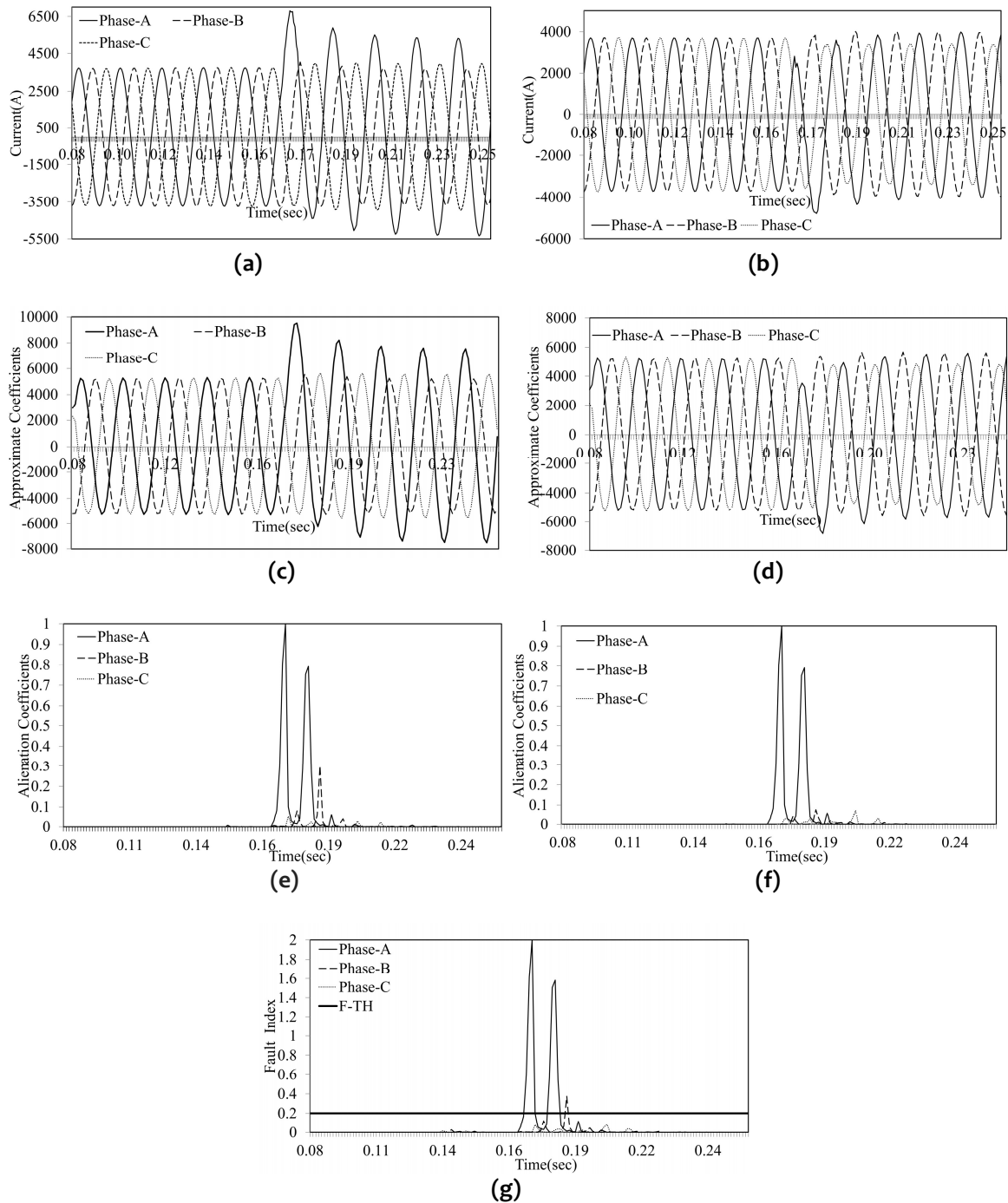


Figure 5.3: Demonstration of AG Fault Detection: (a) Three-phase Current Signals at bus-1, (b) Three-phase Current Signals at bus-2, (c) Approximate Coefficients of bus-1 current signals, (d) Approximate Coefficients of bus-2 current signals, (e) Alienation Coefficients of app. coefficients at Bus-1, (f) Alienation Coefficients of app. coefficients at Bus-2, (g) Fault Index variation with time

Figures 5.4-5.5 depict Fault Index variation of three-phases for BG, CG, AB, BC, AC, ABG, BCG, ACG and ABCG faults. Figures 5.4(a) and 5.4(b) show the fault index variation for BG and CG faults respectively, in which fault index of faulty phase is greater than the threshold and not for the healthy phases. Figures 5.4(c) and 5.4(f) depict the variation of three-phase fault indexes for AB and ABG faults respectively. From these figures, it is evident that phase-A and phase-B have fault index greater than the threshold. Similarly, Figures 5.4 (d) and 5.5 (a) illustrate the fault index variation for BC and BCG faults respectively, from which it can be observed that fault indexes of faulty phases (phase-B & C) are greater than the threshold and not for healthy phase i.e. Phase-A. The fault index variation for AC and ACG faults is shown in Figures 5.4 (e) and 5.5 (b), from these figures it is depicted that fault index for phase-A and phase-C are greater than the threshold whereas for phase-B it remains lower than the threshold, hence the faults are identified as AC and ACG fault respectively. From Figure 5.5 (c), it is evident that all the three phases have fault indexes greater than the threshold, thus it is detected and classified as ABCG fault.

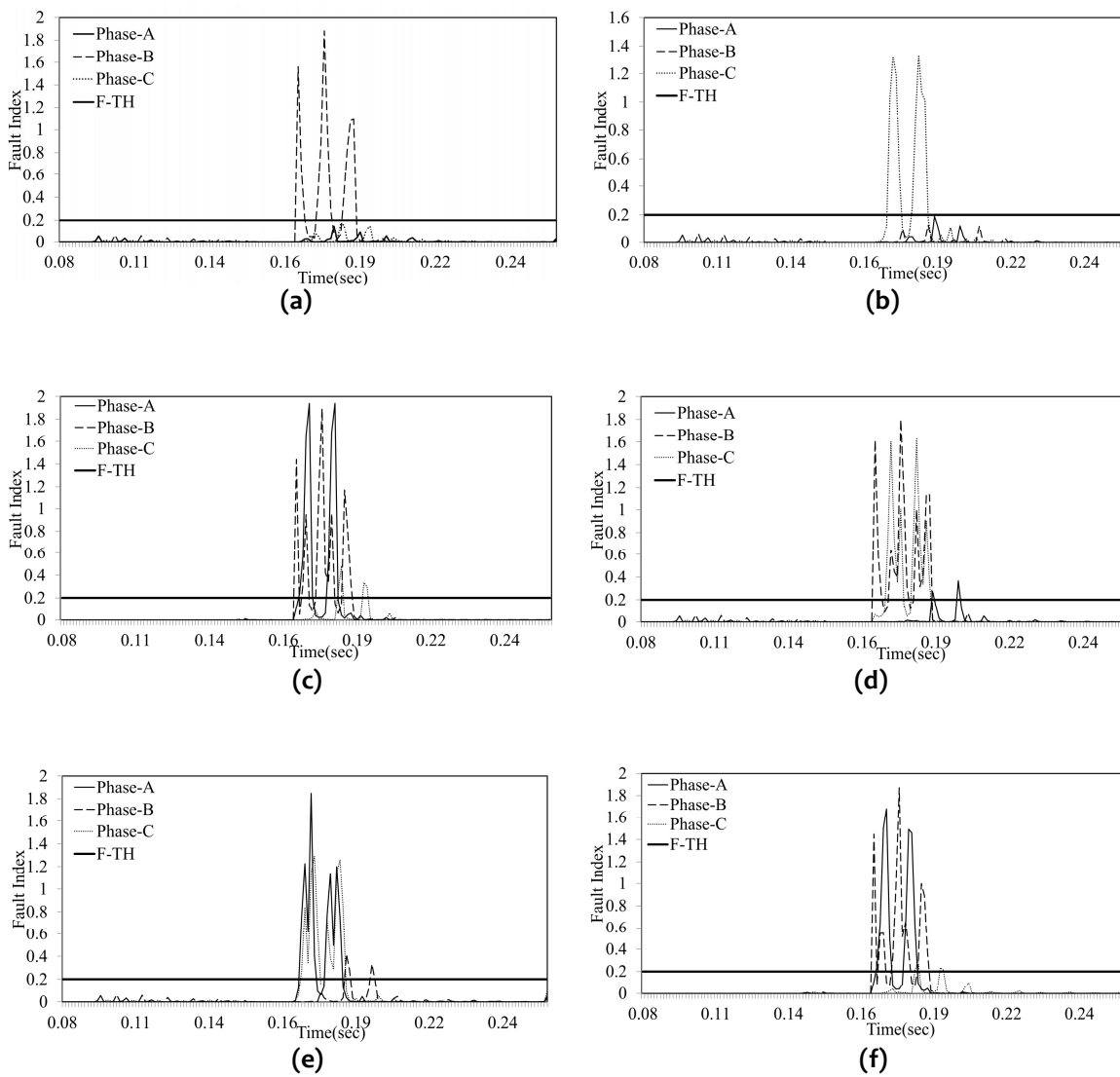


Figure 5.4: Variation of Fault Index with time: (a) BG Fault, (b) CG Fault, (c) AB Fault, (d) BC Fault, (e) AC Fault, (f) ABG Fault,

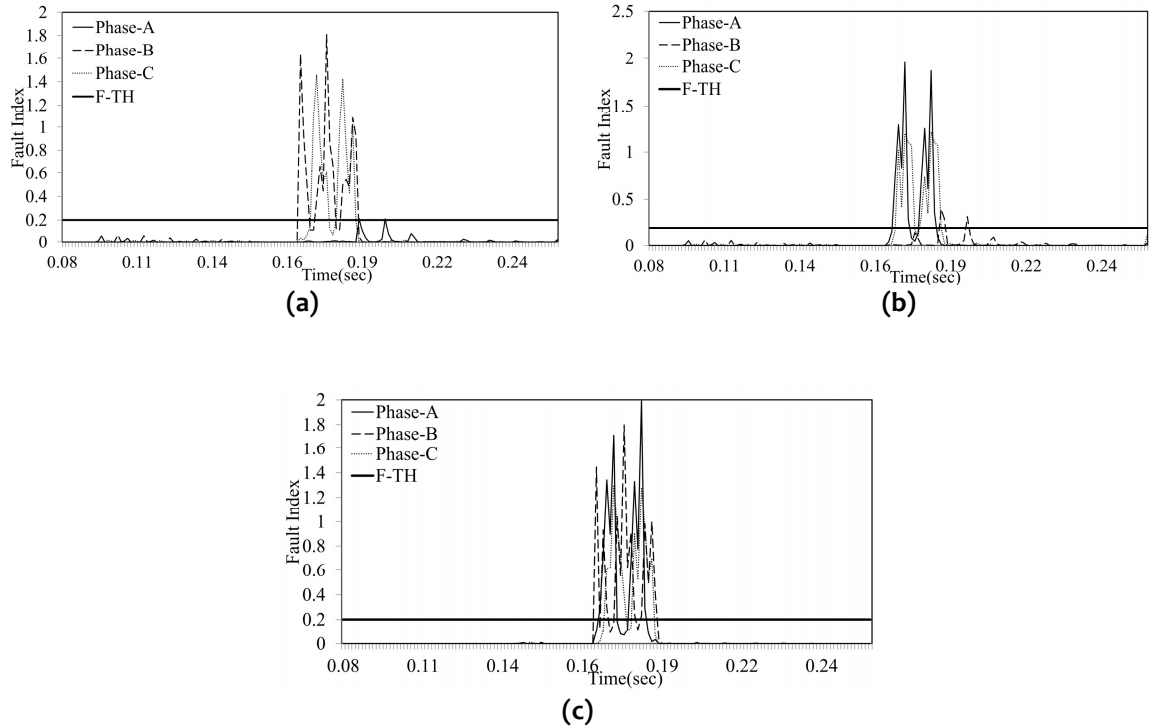


Figure 5.5: Variation of Fault Index with time (a) BCG Fault, (b) ACG Fault, (c) ABCG Fault

However, the discrimination between LL and LLG faults cannot be achieved with the proposed fault index, since the fault indexes of faulty phases in both the cases show no apparent discrimination as shown in Figure 5.4(c) and 5.4(f). To discriminate LLG faults from LL faults, a ground fault index (G-FI) based on zero sequence current is computed by adding the approximate decomposition of zero sequence current over a moving window of quarter cycle. And this resultant G-FI is compared with a threshold which is termed as ground fault threshold (GF-TH = 500) for discrimination purpose. Figure 5.6 depicts the G-FI variation for LL and LLG faults. It is evident from this figure that the fault with ground has G-FI greater than the threshold whereas fault without ground has a lesser value than the threshold.

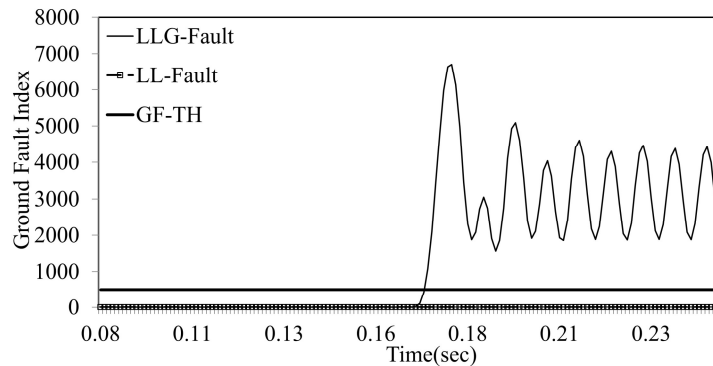


Figure 5.6: Variation of Ground fault index with time

5.3.3 Case Studies

The performance of proposed algorithm has been tested for all the types of faults by varying location, incidence angle and impedance of faults. For the case study of proposed algorithm, different parameters have been varied and are listed in the Table 5.2.

Table 5.2: Case Studies Parameters Variation

S. No.	Parameters	Range of Variation
1	Fault Location	0-230 kms, in steps of 20 kms
2	Fault Incidence Angle	0°-180° in steps of 30°
3	Fault Impedance	5-300 Ω, in steps of 20 Ω
4	Noise Contamination	10-100 dB, in steps of 10 dB
5	Load Switching	10% and 20 % load
6	Sampling Frequency	0.96 kHz, 1.92 kHz, 3.84 kHz and 7.68 kHz
7	STATCOM Control Strategy	Var Control ($Q_{ref.}$ fixed), Var Control ($I_{qref.}$ fixed), Voltage Regulation Control
8	STATCOM Location	At middle of the line and at receiving end

(a) Effect of Fault Location

The post fault current transients are largely dependent on fault locations. Hence, there is a need to test the algorithm at various fault locations to establish its performance. For this purpose all the types of faults have been simulated for every 20 kms along the length of the line. Figure 5.7(a) illustrates variation of fault index with distance for AG fault. It is observed that fault index value of phase-A is more than the threshold and those of healthy phases (B & C) are less than the threshold. It is found that the variation of fault indexes of phases-A and B are always higher than the threshold for AB and ABG faults as shown in Figures 5.7(b) and 5.7(c) respectively, at all the fault locations but the fault index of phase-C remains less than the threshold. From Figure 5.7(d), it is evident that the fault indexes of all the three phases remain greater than the threshold for ABCG fault at various locations. Thus, the proposed algorithm is not affected by variations in fault location.

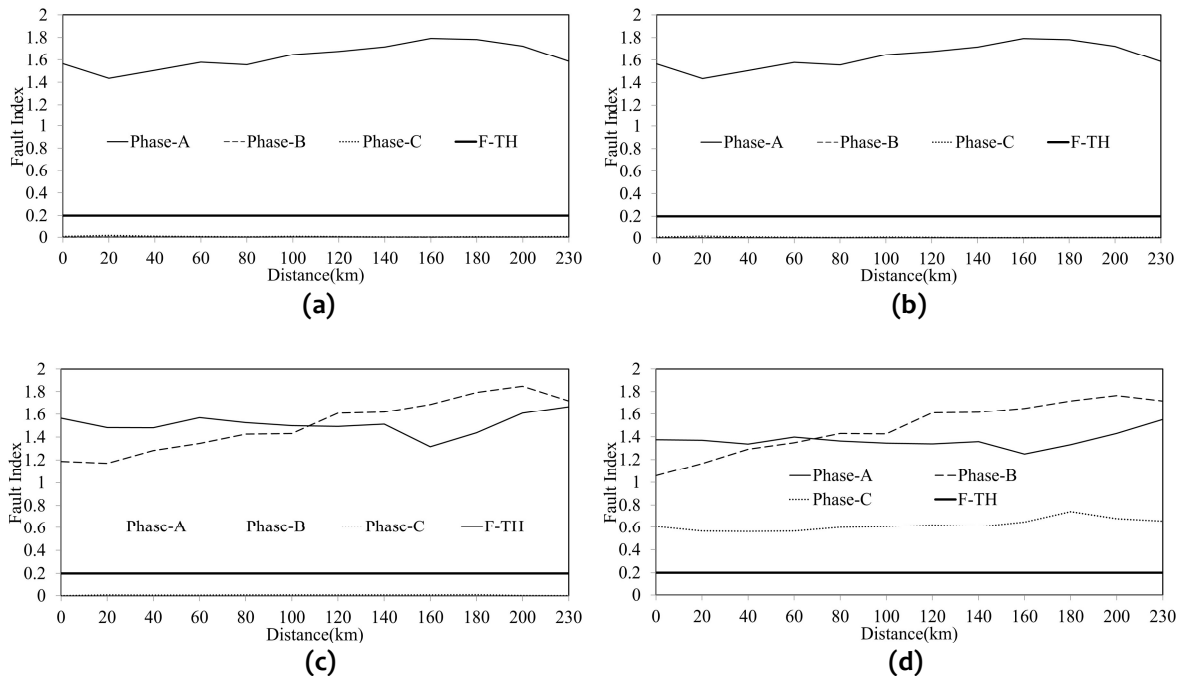


Figure 5.7: Variation of fault index with distance: (a) AG Fault, (b) AB Fault, (c) ABG Fault, (d) ABCG Fault

(b) Effect of Fault Incidence Angle

The post fault current transients are also greatly affected by fault incipient angles. Hence, the proposed algorithm has been tested for its effectiveness with variations in fault incidence angle. The range of variation in fault incidence angle is from 0° to 180° in steps of 30° since

transients obtained from 180° to 360° are found to be similar to those obtained from 0° to 180°. From Figure 5.8(a), it can be observed that the fault index of phase-A is always greater the threshold value, indicating an AG fault. However, fault indexes of other two phases remains less than the threshold. The fault index variations of phase-A and B, for AB and ABG faults, are presented in Figures 5.8(b) and 5.8(c). From these figure, it can be observed that fault indexes of phase-A and B are always greater than the threshold irrespective of fault incidence angle. The fault indexes of all the three phases, in case of ABCG fault, remain higher than the threshold value for different incidence angles, as illustrated in Figure 5.8(d). Tables: 5.3 to 5.12 demonstrate the successful performance of proposed algorithm for various faults at different locations and with variations in incidence angle.

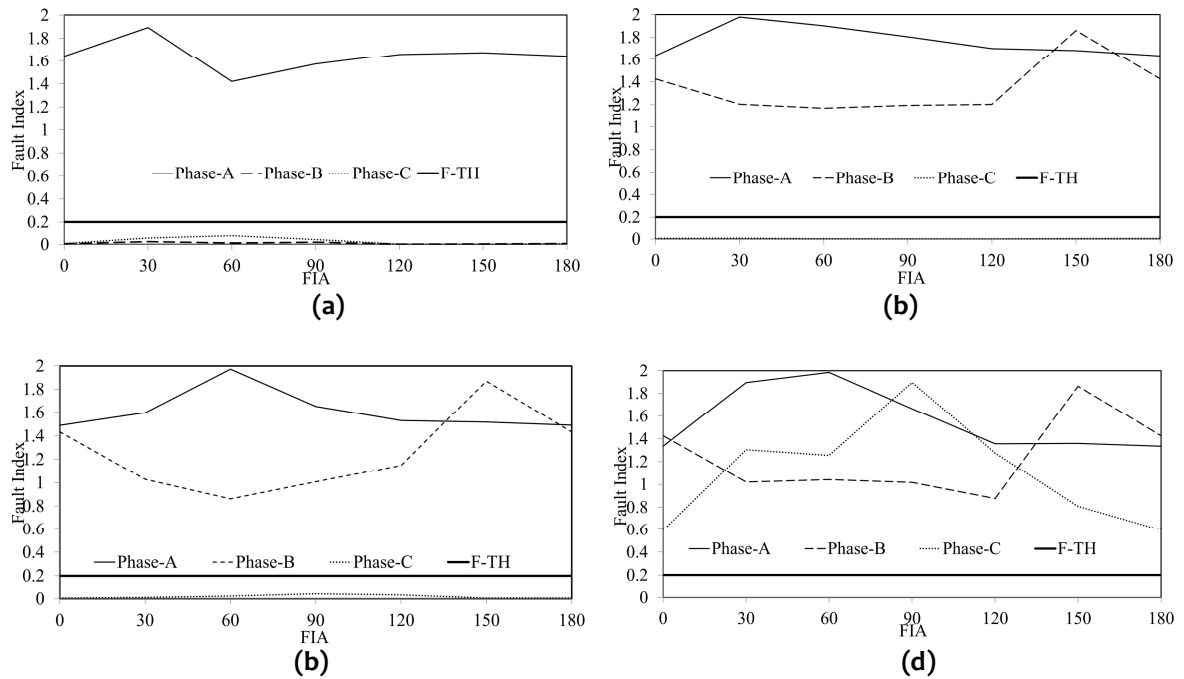


Figure 5.8: Variation of fault index for varying fault incidence angle (FIA): (a) AG Fault, (b) AB Fault, (c) ABG Fault, (d) ABCG Fault

Table 5.3: Fault Index Variation for AG Fault

FIA	0			30			60			90			120			150		
	A	B	C	A	B	C	A	B	C	A	B	C	A	B	C	A	B	C
20	1.43	0.00	0.01	1.41	0.03	0.03	1.46	0.12	0.12	1.47	0.14	0.02	1.48	0.09	0.00	1.48	0.13	0.00
40	1.51	0.00	0.01	1.47	0.03	0.02	1.50	0.08	0.16	1.52	0.16	0.04	1.54	0.07	0.00	1.54	0.04	0.00
60	1.58	0.00	0.01	1.50	0.02	0.07	1.54	0.03	0.12	1.54	0.08	0.02	1.59	0.03	0.00	1.58	0.02	0.00
80	1.56	0.00	0.00	1.51	0.08	0.08	1.58	0.04	0.10	1.59	0.04	0.02	1.62	0.01	0.00	1.64	0.01	0.00
100	1.65	0.00	0.01	1.54	0.13	0.04	1.54	0.07	0.12	1.61	0.06	0.04	1.66	0.01	0.00	1.67	0.00	0.00
120	1.68	0.00	0.00	1.68	0.14	0.10	1.52	0.08	0.11	1.56	0.02	0.06	1.68	0.01	0.01	1.72	0.01	0.00
140	1.72	0.00	0.00	1.62	0.11	0.07	1.69	0.08	0.06	1.60	0.02	0.06	1.64	0.02	0.01	1.74	0.01	0.00
160	1.79	0.00	0.00	1.47	0.10	0.06	1.62	0.15	0.16	1.71	0.03	0.03	1.75	0.03	0.01	1.73	0.01	0.00
180	1.78	0.00	0.00	1.61	0.10	0.12	1.60	0.14	0.14	1.63	0.03	0.09	1.81	0.03	0.01	1.74	0.01	0.00
200	1.72	0.00	0.00	1.54	0.09	0.13	1.69	0.10	0.16	1.64	0.06	0.14	1.68	0.06	0.01	1.75	0.01	0.00
220	1.59	0.00	0.01	1.50	0.17	0.12	1.55	0.15	0.18	1.71	0.11	0.18	1.62	0.13	0.01	1.71	0.01	0.00

Table 5.4: Fault Index Variation for BG Fault

FIA	0			30			60			90			120			150		
	A	B	C	A	B	C	A	B	C	A	B	C	A	B	C	A	B	C
20	0.04	1.03	0.01	0.01	1.12	0.18	0.00	1.13	0.17	0.00	1.13	0.12	0.01	1.07	0.02	0.20	0.79	0.01
40	0.08	1.09	0.01	0.01	1.13	0.06	0.00	1.10	0.07	0.00	1.13	0.07	0.07	1.05	0.01	0.18	0.67	0.22
60	0.07	1.29	0.01	0.01	1.11	0.03	0.00	1.11	0.03	0.00	1.11	0.02	0.04	1.08	0.02	0.16	0.68	0.16
80	0.10	1.40	0.01	0.02	1.12	0.03	0.00	1.12	0.01	0.00	1.12	0.01	0.03	1.12	0.04	0.13	0.68	0.11
90	0.17	1.47	0.01	0.01	1.07	0.02	0.00	1.10	0.01	0.00	1.11	0.01	0.08	1.12	0.02	0.14	0.71	0.08
100	0.03	1.56	0.01	0.03	0.90	0.01	0.00	0.99	0.01	0.00	1.01	0.00	0.03	1.11	0.03	0.07	0.76	0.07
120	0.03	1.58	0.00	0.05	0.91	0.03	0.00	0.95	0.01	0.00	0.96	0.00	0.07	1.08	0.03	0.05	0.81	0.07
140	0.01	1.67	0.01	0.07	0.76	0.03	0.00	0.85	0.03	0.00	0.85	0.00	0.08	0.97	0.02	0.18	0.93	0.07
160	0.11	1.64	0.01	0.02	0.68	0.11	0.00	0.72	0.04	0.00	0.74	0.01	0.10	0.84	0.01	0.14	1.05	0.08
180	0.07	1.61	0.01	0.01	0.93	0.25	0.00	0.80	0.09	0.00	0.72	0.01	0.10	0.72	0.00	0.12	1.19	0.13
200	0.11	1.57	0.02	0.08	1.04	0.35	0.00	0.95	0.11	0.00	0.92	0.02	0.18	0.84	0.01	0.15	1.20	0.13
220	0.04	1.03	0.01	0.01	1.12	0.18	0.00	1.13	0.17	0.00	1.13	0.12	0.01	1.07	0.02	0.10	0.79	0.01

Table 5.5: Fault Index Variation for CG Fault

FIA	0			30			60			90			120			150		
	A	B	C	A	B	C	A	B	C	A	B	C	A	B	C	A	B	C
20	0.12	0.00	0.66	0.03	0.03	1.59	0.01	0.02	1.49	0.00	0.06	1.85	0.00	0.01	0.93	0.12	0.00	1.56
40	0.05	0.00	0.59	0.01	0.02	1.58	0.01	0.02	1.55	0.01	0.04	1.79	0.17	0.02	1.04	0.08	0.00	1.56
60	0.02	0.00	0.60	0.01	0.02	1.55	0.02	0.01	1.49	0.00	0.03	1.77	0.09	0.01	0.90	0.07	0.00	1.57
80	0.01	0.00	0.71	0.00	0.01	1.50	0.01	0.01	1.44	0.01	0.02	1.78	0.03	0.02	0.87	0.04	0.00	1.48
90	0.01	0.00	0.83	0.00	0.01	1.43	0.00	0.01	1.37	0.01	0.05	1.82	0.08	0.01	0.96	0.04	0.00	1.40
100	0.00	0.00	1.03	0.00	0.01	1.37	0.00	0.01	1.31	0.00	0.04	1.77	0.04	0.02	1.04	0.04	0.00	1.34
120	0.01	0.00	1.06	0.00	0.01	1.36	0.00	0.01	1.31	0.00	0.02	1.75	0.07	0.03	0.99	0.03	0.00	1.35
140	0.00	0.00	1.04	0.00	0.01	1.32	0.00	0.01	1.32	0.00	0.02	1.71	0.05	0.03	1.10	0.08	0.00	1.37
160	0.04	0.01	0.93	0.01	0.01	1.27	0.00	0.01	1.33	0.01	0.04	1.67	0.08	0.01	0.73	0.02	0.00	1.27
180	0.05	0.02	0.73	0.01	0.01	1.29	0.00	0.01	1.32	0.01	0.05	1.70	0.09	0.01	1.03	0.11	0.01	1.24
200	0.03	0.03	0.65	0.00	0.02	1.28	0.00	0.02	1.27	0.01	0.05	1.68	0.14	0.02	0.99	0.10	0.01	1.22
220	0.12	0.00	0.66	0.03	0.03	1.59	0.01	0.02	1.49	0.00	0.06	1.85	0.00	0.01	0.93	0.12	0.00	1.56

Table 5.6: Fault Index Variation for AB Fault

FIA	0			30			60			90			120			150		
	A	B	C	A	B	C	A	B	C	A	B	C	A	B	C	A	B	C
20	1.79	0.91	0.00	1.83	1.91	0.01	1.86	1.89	0.00	1.87	1.91	0.00	1.85	1.87	0.03	1.82	1.85	0.00
40	1.71	1.27	0.00	1.78	1.85	0.01	1.80	1.89	0.00	1.82	1.92	0.00	1.71	1.92	0.00	1.76	1.88	0.00
60	1.76	1.33	0.00	1.77	1.92	0.01	1.76	1.94	0.00	1.77	1.92	0.00	1.78	1.90	0.00	1.78	1.85	0.00
80	1.68	1.42	0.00	1.69	1.93	0.01	1.71	1.92	0.00	1.73	1.91	0.00	1.74	1.91	0.00	1.70	1.87	0.00
100	1.65	1.42	0.01	1.68	1.92	0.01	1.70	1.90	0.00	1.70	1.92	0.00	1.70	1.92	0.04	1.70	1.87	0.00
120	1.60	1.63	0.01	1.62	1.91	0.01	1.62	1.93	0.00	1.64	1.93	0.00	1.66	1.93	0.00	1.69	1.88	0.00
140	1.63	1.65	0.01	1.62	1.93	0.01	1.65	1.94	0.00	1.64	1.93	0.00	1.64	1.93	0.00	1.58	1.90	0.00
160	1.44	1.70	0.00	1.48	1.88	0.01	1.53	1.88	0.00	1.61	1.91	0.00	1.64	1.95	0.00	1.55	1.93	0.00
180	1.54	1.80	0.00	1.71	1.96	0.01	1.64	1.94	0.00	1.55	1.89	0.00	1.59	1.95	0.00	1.64	1.96	0.00
200	1.70	1.82	0.00	1.43	1.96	0.01	1.57	1.97	0.00	1.68	1.97	0.00	1.58	1.96	0.00	1.65	1.99	0.00
220	1.76	1.58	0.00	1.56	1.93	0.01	1.43	1.97	0.00	1.58	1.98	0.00	1.61	1.97	0.00	1.57	1.99	0.00

Table 5.7: Fault Index Variation for BC Fault

FIA Loca tion	0			30			60			90			120			150		
	A	B	C	A	B	C	A	B	C	A	B	C	A	B	C	A	B	C
20	0.00	1.90	1.58	0.00	1.84	1.61	0.00	1.89	1.62	0.01	1.91	1.96	0.00	1.76	0.98	0.01	1.96	1.02
40	0.00	1.85	1.55	0.00	1.83	1.61	0.00	1.90	1.59	0.01	1.80	1.95	0.00	1.70	1.00	0.01	1.99	0.94
60	0.00	1.81	1.57	0.00	1.85	1.62	0.00	1.81	1.57	0.01	1.75	1.93	0.00	1.79	1.06	0.01	1.95	0.71
80	0.00	1.86	1.66	0.00	1.83	1.63	0.00	1.82	1.58	0.00	1.84	1.92	0.00	1.87	1.26	0.01	1.96	0.59
100	0.00	1.81	1.62	0.00	1.82	1.60	0.00	1.82	1.58	0.00	1.82	1.90	0.01	1.85	1.24	0.01	1.95	0.48
120	0.01	1.80	1.60	0.00	1.80	1.60	0.00	1.80	1.60	0.01	1.80	1.87	0.01	1.79	1.18	0.01	1.92	0.38
140	0.02	1.80	1.61	0.01	1.79	1.61	0.00	1.80	1.61	0.01	1.80	1.87	0.01	1.79	1.17	0.01	1.93	0.38
160	0.02	1.80	1.66	0.01	1.80	1.69	0.00	1.79	1.62	0.00	1.81	1.81	0.01	1.80	1.11	0.01	1.92	0.34
180	0.02	1.78	1.46	0.01	1.78	1.63	0.00	1.79	1.63	0.00	1.80	1.72	0.01	1.76	0.72	0.01	1.92	0.33
200	0.02	1.76	1.56	0.01	1.78	1.51	0.01	1.75	1.65	0.01	1.76	1.77	0.00	1.77	1.00	0.01	1.94	0.36
220	0.02	1.76	1.62	0.01	1.77	1.52	0.00	1.77	1.61	0.00	1.77	1.69	0.00	1.77	0.97	0.01	1.94	0.36

Table 5.8: Fault Index Variation for AC Fault

FIA Loca tion	0			30			60			90			120			150		
	A	B	C	A	B	C	A	B	C	A	B	C	A	B	C	A	B	C
20	1.27	0.08	1.46	1.50	0.10	1.54	1.84	0.02	1.32	1.88	0.01	1.76	1.16	0.00	0.58	1.33	0.11	0.66
40	1.13	0.07	1.47	1.13	0.10	1.42	1.37	0.03	1.23	1.73	0.01	1.79	1.17	0.00	0.66	1.33	0.04	0.71
60	1.16	0.07	1.35	1.27	0.10	1.24	1.48	0.04	1.14	1.16	0.01	1.81	1.17	0.00	0.94	1.28	0.02	0.66
80	1.29	0.07	1.32	1.12	0.11	1.29	1.13	0.05	1.28	1.19	0.01	1.86	1.16	0.00	1.01	1.30	0.02	0.87
100	1.46	0.07	1.32	1.37	0.11	1.31	1.20	0.08	1.30	1.17	0.01	1.84	1.18	0.00	1.08	1.31	0.01	1.01
120	1.85	0.09	1.29	1.75	0.12	1.27	1.42	0.09	1.29	1.15	0.01	1.81	1.32	0.01	1.16	1.34	0.03	1.03
140	1.94	0.09	1.29	1.79	0.12	1.34	1.86	0.08	1.29	1.16	0.01	1.82	1.34	0.01	1.18	1.42	0.03	1.02
160	1.99	0.10	1.27	1.99	0.11	1.21	2.00	0.06	1.20	1.08	0.01	1.76	1.40	0.01	1.20	1.45	0.06	1.00
180	1.76	0.10	1.26	1.63	0.10	1.25	1.75	0.05	1.12	1.10	0.01	1.61	1.15	0.06	0.89	1.34	0.07	1.03
200	1.36	0.09	1.23	1.00	0.08	1.29	1.72	0.04	1.21	1.63	0.01	1.65	1.51	0.16	0.93	1.19	0.13	1.03
220	1.15	0.07	1.26	1.16	0.07	1.29	1.58	0.03	1.28	1.45	0.01	1.65	1.64	0.11	0.96	1.45	0.12	1.04

Table 5.9: Fault Index Variation for ABG Fault

FIA Loca tion	0			30			60			90			120			150		
	A	B	C	A	B	C	A	B	C	A	B	C	A	B	C	A	B	C
20	1.48	1.17	0.01	1.46	1.91	0.24	1.49	1.87	0.18	1.50	1.92	0.12	1.52	1.85	0.01	1.49	1.87	0.01
40	1.48	1.28	0.00	1.49	1.82	0.09	1.51	1.88	0.16	1.55	1.91	0.09	1.53	1.85	0.02	1.50	1.90	0.01
60	1.57	1.34	0.01	1.53	1.91	0.04	1.52	1.93	0.06	1.53	1.91	0.05	1.55	1.86	0.01	1.58	1.87	0.01
80	1.53	1.43	0.01	1.48	1.93	0.02	1.51	1.91	0.04	1.54	1.88	0.03	1.55	1.87	0.03	1.52	1.88	0.01
100	1.50	1.43	0.01	1.50	1.90	0.01	1.51	1.88	0.03	1.54	1.88	0.04	1.54	1.88	0.04	1.53	1.88	0.01
120	1.49	1.61	0.01	1.47	1.88	0.01	1.47	1.90	0.03	1.48	1.91	0.04	1.48	1.91	0.04	1.53	1.89	0.01
140	1.51	1.62	0.01	1.47	1.89	0.02	1.52	1.90	0.02	1.52	1.89	0.04	1.49	1.90	0.04	1.41	1.90	0.01
160	1.32	1.69	0.01	1.34	1.86	0.03	1.38	1.85	0.05	1.47	1.87	0.03	1.54	1.90	0.03	1.45	1.92	0.01
180	1.44	1.79	0.01	1.59	1.90	0.04	1.52	1.90	0.05	1.44	1.85	0.08	1.48	1.89	0.02	1.55	1.93	0.01
200	1.61	1.85	0.00	1.30	1.89	0.10	1.45	1.89	0.10	1.59	1.88	0.10	1.48	1.87	0.02	1.55	1.94	0.02
220	1.67	1.72	0.00	1.43	1.84	0.17	1.31	1.88	0.17	1.50	1.88	0.13	1.51	1.87	0.02	1.45	1.94	0.01

Table 5.10: Fault Index Variation for BCG Fault

FIA Location	0			30			60			90			120			150		
	A	B	C	A	B	C	A	B	C	A	B	C	A	B	C	A	B	C
20	0.18	1.02	1.08	0.04	0.98	1.50	0.01	0.91	1.45	0.00	0.98	1.95	0.00	1.10	1.03	0.03	0.97	0.30
40	0.04	1.17	1.08	0.04	0.98	1.51	0.01	1.03	1.46	0.00	1.01	1.94	0.02	0.98	1.16	0.03	0.95	1.51
60	0.03	1.32	1.08	0.02	1.03	1.51	0.01	1.03	1.43	0.00	1.04	1.92	0.01	0.92	1.19	0.02	0.94	1.35
80	0.04	1.43	1.10	0.03	0.93	1.52	0.01	1.00	1.44	0.00	1.04	1.92	0.01	0.85	1.39	0.02	1.03	1.52
90	0.05	1.46	1.10	0.00	0.87	1.44	0.00	0.87	1.42	0.00	1.02	1.90	0.01	0.69	1.39	0.02	1.07	1.44
100	0.01	1.63	1.09	0.04	0.72	1.42	0.00	0.78	1.42	0.00	0.93	1.85	0.01	0.84	1.39	0.02	1.19	1.41
120	0.01	1.64	1.09	0.04	0.76	1.46	0.00	0.76	1.42	0.00	0.92	1.85	0.01	0.84	1.39	0.03	1.24	1.47
140	0.01	1.70	1.12	0.04	0.61	1.51	0.01	0.75	1.44	0.00	0.82	1.80	0.02	0.89	1.36	0.04	1.30	1.40
160	0.03	1.80	1.11	0.01	0.59	1.44	0.00	0.72	1.44	0.01	0.79	1.73	0.07	0.97	1.14	0.06	1.31	1.29
180	0.02	1.83	1.01	0.02	0.66	1.33	0.01	0.72	1.37	0.01	0.80	1.75	0.16	1.05	1.07	0.11	1.30	1.45
200	0.12	1.88	0.86	0.09	0.76	1.30	0.01	0.83	1.30	0.00	0.88	1.73	0.25	1.06	1.03	0.20	1.27	1.43
220	0.18	1.02	1.08	0.04	0.98	1.50	0.01	0.91	1.45	0.00	0.98	1.95	0.00	1.10	1.03	0.03	0.97	0.30

Table 5.11: Fault Index Variation for ACG Fault

FIA Location	0			30			60			90			120			150		
	A	B	C	A	B	C	A	B	C	A	B	C	A	B	C	A	B	C
20	1.30	0.04	0.71	1.93	0.03	1.36	1.76	0.02	1.37	0.55	0.03	1.91	1.32	0.05	1.04	1.33	0.01	1.26
40	1.25	0.05	0.58	1.92	0.02	1.36	1.80	0.01	1.24	0.40	0.01	1.91	1.30	0.03	1.01	1.33	0.00	1.23
60	1.30	0.01	0.76	1.93	0.01	1.22	1.81	0.01	1.17	0.49	0.01	1.89	1.30	0.01	0.93	1.28	0.00	1.24
80	1.28	0.01	0.90	1.84	0.01	1.13	1.68	0.01	1.15	0.32	0.01	1.89	1.28	0.01	1.14	1.30	0.00	1.28
90	1.30	0.01	0.96	1.92	0.01	1.26	1.74	0.01	1.18	0.51	0.01	1.86	1.29	0.00	1.19	1.31	0.00	1.18
100	1.29	0.01	1.02	1.95	0.01	1.25	1.82	0.01	1.19	0.39	0.01	1.82	1.32	0.00	1.27	1.34	0.00	1.18
120	1.33	0.01	1.02	1.99	0.01	1.21	1.99	0.01	1.16	0.40	0.01	1.83	1.30	0.01	1.30	1.42	0.00	1.23
140	1.38	0.01	1.03	1.81	0.01	1.17	1.98	0.02	1.17	0.46	0.01	1.78	1.41	0.00	1.33	1.45	0.00	1.22
160	1.40	0.04	1.02	1.23	0.04	1.23	1.83	0.02	1.20	0.48	0.01	1.65	1.16	0.00	1.19	1.34	0.00	1.17
180	1.40	0.06	1.02	1.30	0.06	1.24	1.97	0.04	1.25	0.39	0.01	1.68	1.45	0.01	1.14	1.19	0.00	1.25
200	1.40	0.06	1.00	1.35	0.05	1.24	1.98	0.03	1.30	0.32	0.01	1.67	1.63	0.01	1.02	1.45	0.01	1.27
220	1.30	0.04	0.71	1.93	0.03	1.36	1.76	0.02	1.37	0.55	0.03	1.91	1.32	0.05	1.04	1.33	0.01	1.26

Table 5.12: Fault Index Variation for ABCG Fault

FIA Location	0			30			60			90			120			150		
	A	B	C	A	B	C	A	B	C	A	B	C	A	B	C	A	B	C
20	1.37	1.16	0.56	1.83	1.83	1.37	1.95	1.83	1.39	1.38	1.87	1.95	1.39	1.78	0.97	1.38	1.88	0.59
40	1.34	1.29	0.56	1.75	1.77	1.37	1.80	1.84	1.31	1.38	1.83	1.94	1.38	1.76	0.99	1.36	1.91	0.76
60	1.40	1.35	0.56	1.73	1.85	1.31	1.89	1.85	1.23	1.36	1.80	1.91	1.37	1.81	1.10	1.38	1.87	0.65
80	1.36	1.43	0.60	1.90	1.85	1.27	1.98	1.83	1.25	1.37	1.84	1.90	1.36	1.86	1.34	1.35	1.88	0.58
100	1.34	1.42	0.60	1.86	1.83	1.31	1.99	1.82	1.26	1.35	1.83	1.87	1.36	1.85	1.38	1.37	1.88	0.82
120	1.34	1.61	0.62	1.85	1.82	1.31	1.99	1.84	1.28	1.33	1.83	1.83	1.36	1.82	1.41	1.37	1.86	0.70
140	1.36	1.62	0.61	1.99	1.83	1.30	1.97	1.84	1.26	1.34	1.83	1.84	1.37	1.82	1.43	1.35	1.87	0.67
160	1.25	1.65	0.65	1.85	1.82	1.31	1.90	1.82	1.28	1.32	1.84	1.80	1.44	1.84	1.43	1.39	1.87	0.73
180	1.33	1.72	0.74	1.62	1.84	1.31	1.77	1.84	1.31	1.28	1.83	1.68	1.29	1.83	1.06	1.39	1.89	0.67
200	1.43	1.76	0.68	1.46	1.84	1.29	1.95	1.85	1.33	1.59	1.84	1.71	1.45	1.84	0.98	1.34	1.93	0.79
220	1.55	1.72	0.66	1.43	1.82	1.28	1.97	1.84	1.33	1.43	1.84	1.70	1.54	1.84	0.96	1.37	1.94	0.84

(c) Effect of Fault Impedance

Faults with high impedances are difficult to detect due to low post-fault currents, if the sensitivity of the relay is poor. To establish the sensitivity of the proposed protection scheme, fault impedances of different magnitudes (from 5Ω to 100Ω) have been introduced in various types of faults. Figures 5.9-5.10 illustrate the fault index variation of all the three-phases for different types of faults, for a fault impedance of 100Ω . Figure 5.9(a) depicts that the fault index of phase-A is higher than the threshold and for other phases it is less than the threshold at all the locations hence it is detected as AG fault. Figures 5.9(b) and 5.9(c) show the fault index variation for BG and CG faults respectively, in which fault index of faulty phase is greater than the threshold and not for the healthy phases. Figures 5.9(d) and 5.10(a) depict the variation of three-phase fault indexes for AB and ABG faults respectively. Form these figures, it is evident that phase-A and phase-B have fault index greater than the threshold. Similarly, Figures 5.9(e) and 5.10(b) illustrate the fault index variation for BC and BCG faults respectively, from which it can be observed that fault indexes of faulty phases (phase-B & C) are greater than the threshold and not for healthy phase i.e. Phase-A.

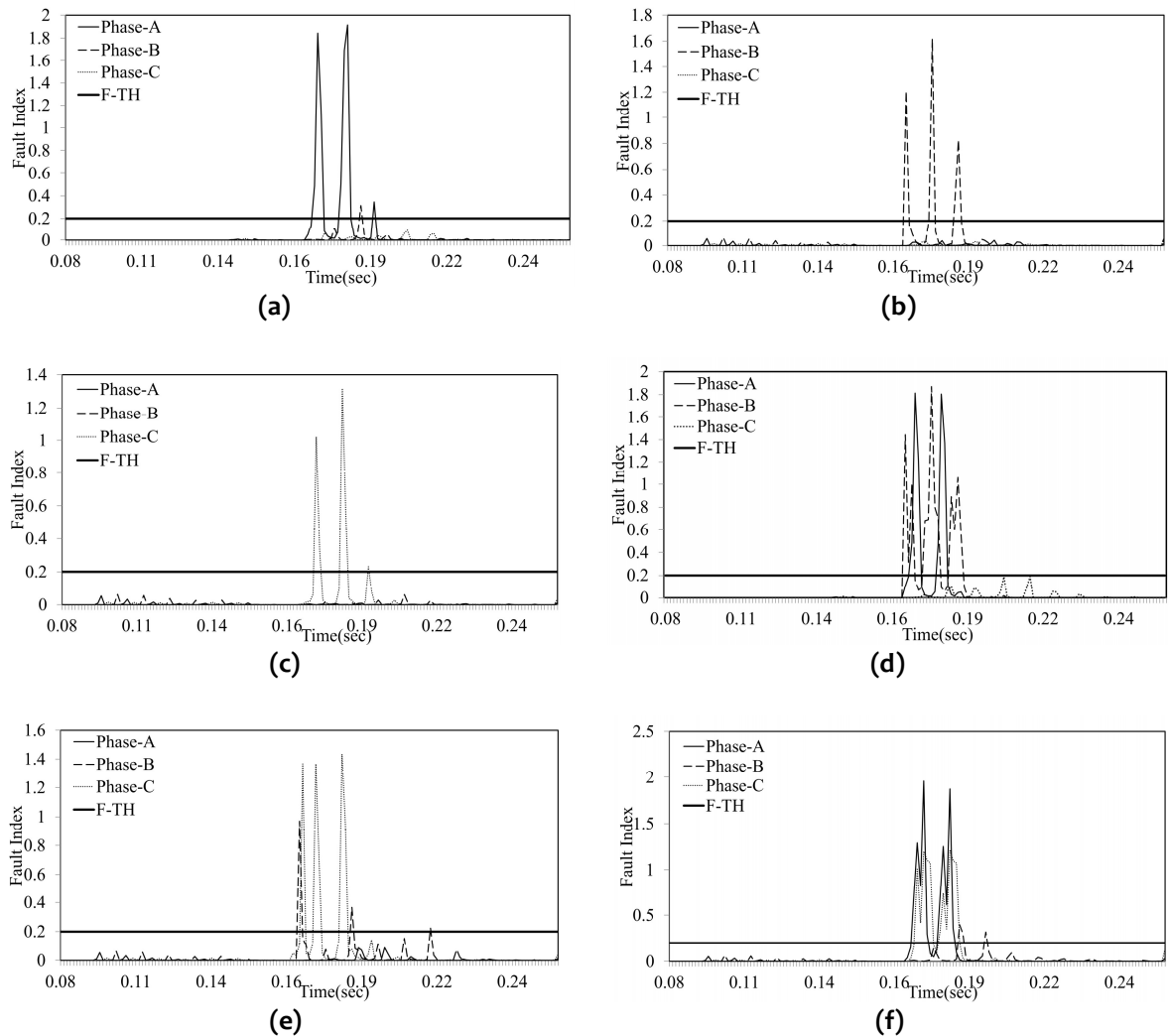


Figure 5.9: Variation of fault index for fault impedance of 100Ω : (a) AG Fault, (b) BG Fault, (c) CG Fault, (d) AB Fault, (e) BC Fault, (f) AC Fault

The fault index variation for AC and ACG faults is shown in Figures 5.9(f) and 5.10(c), from these figures it is depicted that fault index for phase-A and phase-C are greater than the threshold whereas for phase-B it remains lower than the threshold, hence fault are

identified as AC and ACG fault respectively. Figure 5.10(d) shows that for all the three phases, fault index is greater than the threshold, hence it is detected as three phase to ground (ABCG) fault. Thus, it is evident that the fault impedance has no effect on proposed algorithm.

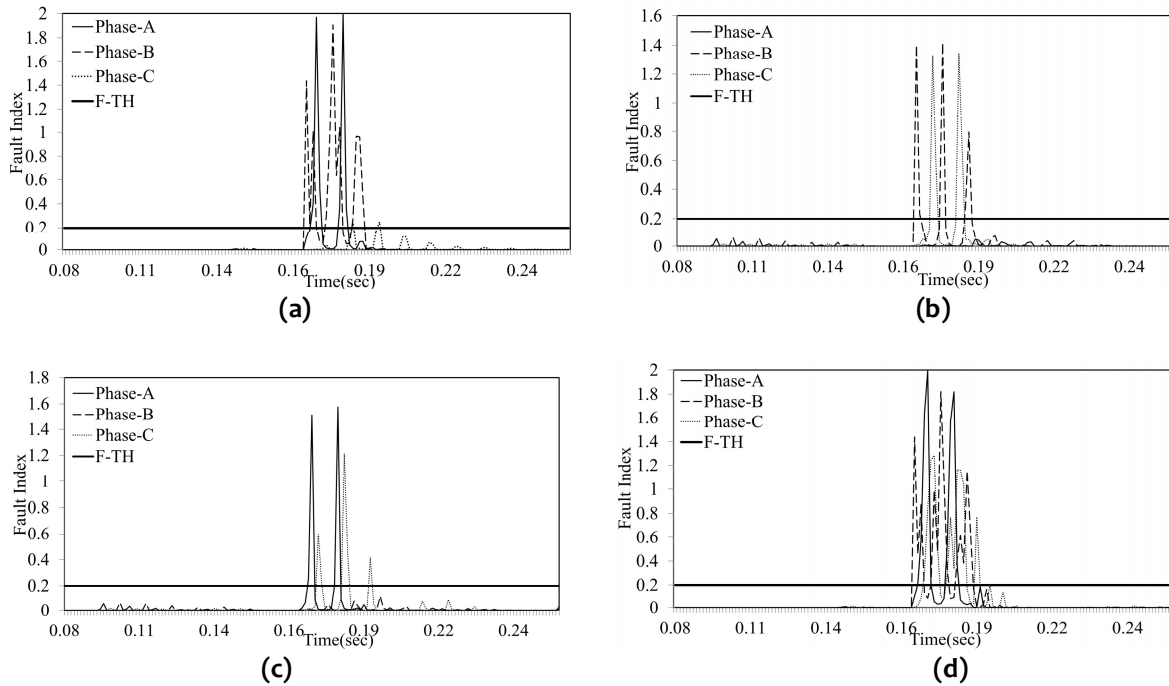


Figure 5.10: Variation of fault index for fault impedance of 100Ω : (a) ABG Fault, (b) BCG Fault, (c) ACG Fault, (d) ABCG Fault

(d) Effect of STATCOM Location

The location of STATCOM affects the magnitude and transients of bus-currents. Hence, the performance of the proposed algorithm is verified by changing the STATCOM location to receiving end (Bus-2). Figures 5.11(a-d) illustrate the variation of three-phase fault index for AG, AB, ABG and ABCG faults respectively. From these figures, it can be observed that the fault index of faulty phases exceed the threshold value, whereas those of healthy phases possess a lower value the threshold. Hence, it can be established that the location of STATCOM does not affect the performance of the proposed algorithm.

(e) Performance in Noisy Environment

To examine the noise influence on proposed algorithm, the current signals are contaminated with different levels of noise (10dB-50dB). Figure 5.12 depicts variation of three-phase fault index for different types of faults, with 10dB white Gaussian noise. Figure 5.12(a) depicts variation of fault index for AG fault. The fault index of phase-A is greater than the threshold and that of other phases is less than the threshold, thus illustrating AG fault. Figures 5.12(b) and 5.12 (c) illustrate that for phase-A and phase-B, fault index is greater than the threshold and not for phase-C, and hence the fault is detected as AB and ABG fault. Figure 5.12(d) shows that for all the three phases, fault index is greater than the threshold. Hence it is detected as ABCG fault. Thus, it is evident that presence of noise in the current signals has no effect on proposed algorithm.

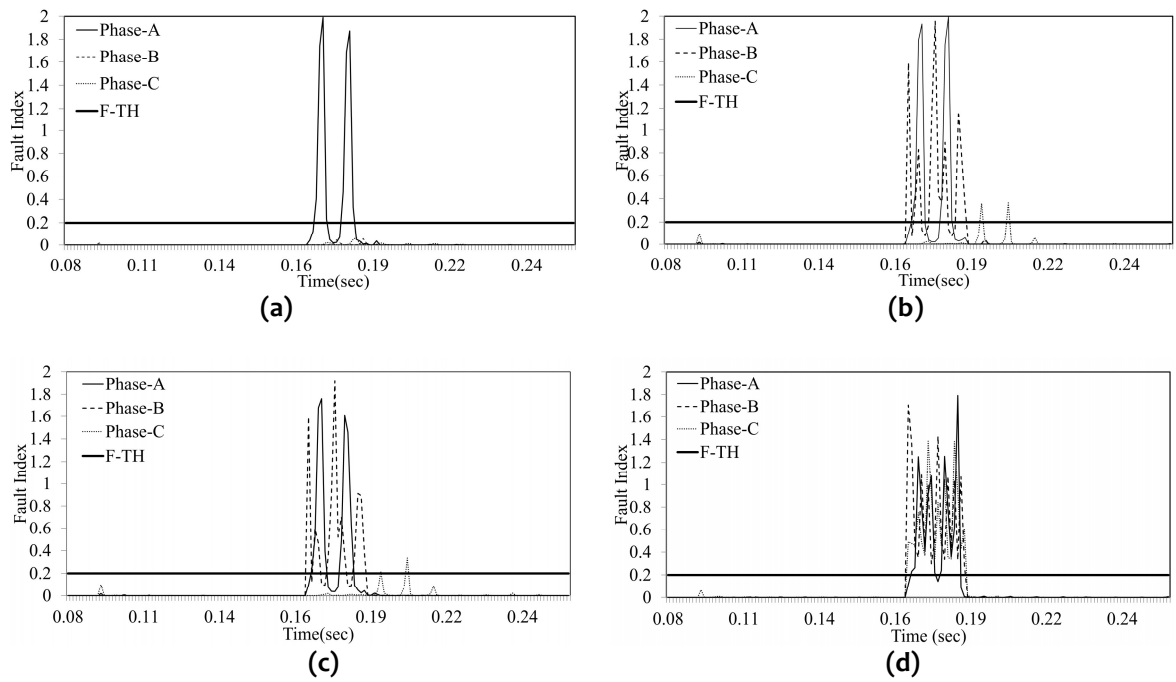


Figure 5.11: FI variation for STATCOM installed at bus-2: (a) AG Fault, (b) AB Fault, (c) ABG Fault, (d) ABCG Fault.

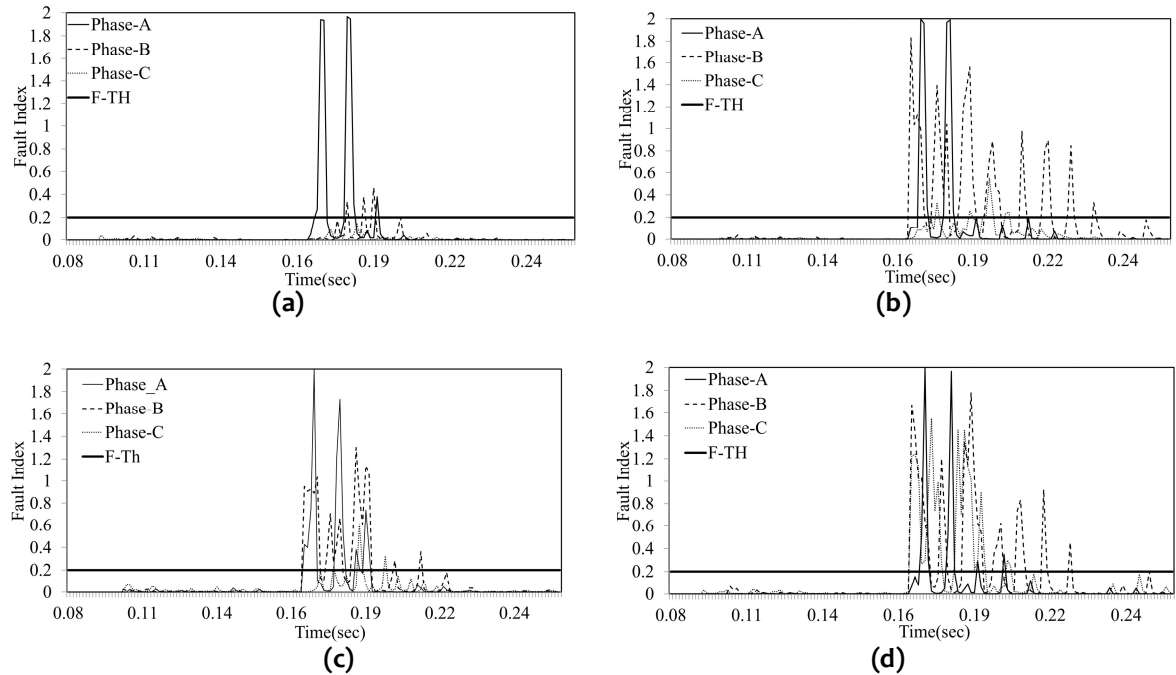


Figure 5.12: FI variation for Noisy environment: (a) AG Fault, (b) AB Fault, (c) ABG Fault, (d) ABCG Fault

(f) Effect of Loading

The proposed algorithm has been tested with load switching. It has been observed that for 10% and 20% load switching, the maximum values of fault index for phase-A, phase-B and phase-C are 0.04, 0.02 and 0.08 respectively, which are well below the threshold value.

(g) Effect of Power-Flow Direction

To consider the effect of power-flow direction in the proposed algorithm, it has been tested on reverse power flow condition. Since the proposed scheme is making use of data from both the buses, the obtained results corresponding to reverse power-flow are same as before.

(h) Effect of Sampling Frequency

The algorithm has been tested with sampling frequency of 0.96 kHz, 1.92 kHz, 3.84 kHz and 7.68 kHz, it has been observed that increase in frequency has no considerable improvement in terms of accuracy and speed of proposed protection scheme. However the reduction in sampling frequency increases the detection time and error.

5.3.4 Location of Fault

Estimation of fault location has been carried out, followed by fault detection and classification, using Artificial Neural Network. A multi-layer feed-forward neural network, whose structure is shown in Figure 5.13, is used to locate the fault. The details related to structure of ANN are presented in Table 5.13.

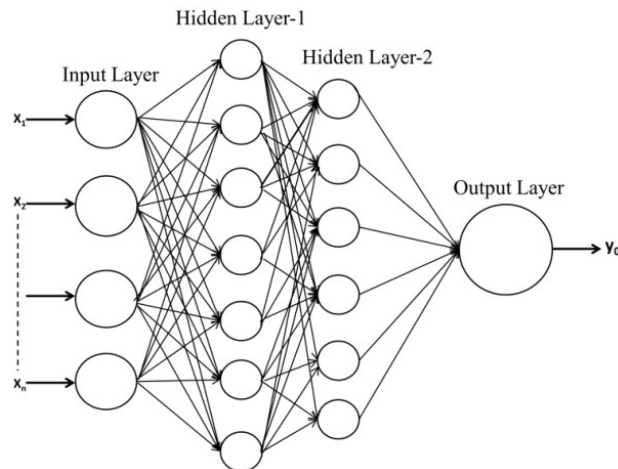


Figure 5.13: ANN Structure

Table 5.13 Details of ANN Structure

Layer	No. of Neurons	Transfer Function
Input Layer	48	Purelin
Hidden Layer-1	24	Log-sigmoid
Hidden Layer-2	8	Log-sigmoid
Output	1	Purelin

Table 5.14 Details of Simulated Data

No. of Fault Locations	24 (for 230 km line, at a steps of 10 kms)
Types of Faults	10 (AG, BG, CG, AB, BC, AC, ABG, BCG, ACG, ABCG)
Fault Impedances	4 (0, 5, 10, 15 Ω)
Fault Incidence Angle	6 (0, 30, 60, 90, 120, 150)
Total number of data sets obtained	$24 * 10 * 4 * 6 = 5760$

The input is fed from 48 approximate coefficients of three-phase voltage and current signals of both the ends of the line. The output of ANN will be fault location (in kms) from bus-1. Each signal yields 4 approximate coefficients, thus total number of approximate coefficients

fed can be given by $[2(\text{buses}) * \{3(\text{phase voltage}) + 3(\text{phase current})\}] * 4 = 48$ coefficients. The details of simulated data, obtained by a number of case studies are listed in Tables 5.14 and 5.15.

Table 5.15 Details of ANN training and testing are as follows:

Training Data Sets	(70%) = 4032
Validation Data Sets	(15%) = 864
Testing Data Sets	(15%) = 864

Table 5.16: Fault Locations Results for AG, BG, CG, AB and BC Faults

S.No	Fault type	FIA	Fault Imp.	Actual Location	ANN Location	% Error
1	AG	0	0	22	21.07	0.41
2	AG	0	0	143	142.41	0.26
3	AG	0	15	47	49.31	1.00
4	AG	0	15	166	166.39	0.17
5	AG	90	0	87	89.42	1.05
6	AG	90	0	207	209.94	1.28
7	AG	90	15	65	67.22	0.96
8	AG	90	15	135	135.20	0.09
9	BG	0	0	47	46.86	0.06
10	BG	0	0	166	166.64	0.28
11	BG	0	10	65	64.92	0.03
12	BG	0	10	195	194.34	0.29
13	BG	60	0	22	22.02	0.01
14	BG	60	0	135	137.01	0.87
15	BG	60	10	87	90.00	1.30
16	BG	60	10	207	202.11	2.12
17	CG	0	0	65	63.20	0.78
18	CG	0	0	195	197.11	0.92
19	CG	0	5	87	87.32	0.14
20	CG	0	5	207	208.56	0.68
21	CG	120	0	47	44.08	1.27
22	CG	120	0	143	142.96	0.02
23	CG	120	5	22	17.91	1.78
24	CG	120	5	166	169.69	1.60
25	AB	0	0	87	85.59	0.61
26	AB	0	0	207	208.81	0.79
27	AB	0	15	22	21.45	0.24
28	AB	0	15	135	134.36	0.28
29	AB	30	0	65	65.93	0.40
30	AB	30	0	166	167.99	0.87
31	AB	30	15	47	51.73	2.06
32	AB	30	15	143	142.80	0.09
33	BC	0	0	22	21.75	0.11
34	BC	0	0	135	133.87	0.49
35	BC	0	10	47	47.39	0.17
36	BC	0	10	207	201.79	2.27
37	BC	90	0	87	82.30	2.04
38	BC	90	0	195	191.87	1.36
39	BC	90	10	65	62.47	1.10
40	BC	90	10	166	165.58	0.18

Tables 5.16-5.17 demonstrate the accuracy of proposed algorithm using ANN. It can also be observed that maximum and average errors in locating the faults are 2.03% and 0.87% respectively. The error in fault location can be calculated as follows:

$$\%Error = \frac{|NNDistance - ActualDistance|}{L} * 100$$

Table 5.17: Fault Locations Results for AC, ABG, BCG, ACG and ABC Faults

S.No	Fault type	FIA	Fault Imp.	Actual Location	ANN Location	% Error
1	AC	0	0	47	41.40	2.43
2	AC	0	0	143	147.34	1.89
3	AC	0	5	65	64.48	0.22
4	AC	0	5	195	193.26	0.76
5	AC	120	0	22	22.22	0.10
6	AC	120	0	207	202.05	2.15
7	AC	120	5	87	86.90	0.05
8	AC	120	5	135	136.85	0.81
9	ABG	0	0	65	62.97	0.88
10	ABG	0	0	166	167.99	0.87
11	ABG	0	10	87	85.75	0.54
12	ABG	0	10	135	134.28	0.31
13	ABG	150	0	47	44.48	1.10
14	ABG	150	0	143	142.98	0.01
15	ABG	150	10	22	22.25	0.11
16	ABG	150	10	207	208.44	0.63
17	BCG	0	0	87	86.37	0.27
18	BCG	0	0	195	199.31	1.87
19	BCG	0	5	22	20.06	0.84
20	BCG	0	5	207	200.48	2.83
21	BCG	30	0	65	62.11	1.26
22	BCG	30	0	143	145.91	1.26
23	BCG	30	5	47	46.42	0.25
24	BCG	30	5	166	166.93	0.41
25	ACG	0	0	22	23.42	0.62
26	ACG	0	0	207	210.26	1.42
27	ACG	0	15	47	43.98	1.31
28	ACG	0	15	195	195.26	0.11
29	ACG	90	0	65	64.34	0.29
30	ACG	90	0	166	165.95	0.02
31	ACG	90	15	22	24.67	1.16
32	ACG	90	15	135	139.60	2.00
33	ABC	0	0	47	44.99	0.87
34	ABC	0	0	195	198.32	1.44
35	ABC	0	10	22	20.82	0.51
36	ABC	0	10	207	208.03	0.45
37	ABC	60	0	65	68.20	1.39
38	ABC	60	0	135	131.53	1.51
39	ABC	60	10	87	86.71	0.12
40	ABC	60	10	166	168.77	1.20

5.3-5 Comparison of Performances

In this section, efforts have been made to prove the ability of algorithm to detect and classify the faults, even in the absence of STATCOM (due to maintenance or outage). For this purpose, STATCOM has been disconnected from the transmission line and various types of faults have been simulated. Table 5.18 compares the performance of proposed protection scheme with and without presence of STATCOM. From this table, it can be established that the presence and absence of FACTS device has no effect on algorithm.

Table 5.18: Fault index variation in presence and absence of STATCOM

S.No	Fault Type	Phase-A		Phase-B		Phase-C	
		Without STATCOM	With STATCOM	Without STATCOM	With STATCOM	Without STATCOM	With STATCOM
1	AG	1.79	1.65	0.01	0.01	0.00	0.01
	BG	0.12	0.17	1.42	1.47	0.01	0.01
3	CG	0.01	0.01	0.00	0.00	0.90	0.83
4	AB	1.82	1.96	1.48	1.78	0.00	0.01
5	BC	0.00	0.00	1.36	1.42	0.80	0.74
6	AC	1.40	1.19	0.00	0.00	1.00	1.01
7	ABG	1.68	1.72	1.49	1.43	0.00	0.01
8	BCG	0.03	0.05	1.47	1.46	1.10	1.10
9	ACG	1.49	1.30	0.01	0.01	0.97	0.96
10	ABC	1.52	1.33	1.49	1.43	0.63	0.62

5.4 TCSC-COMPENSATED TRANSMISSION SYSTEM

5.4.1 System Model and Parameters

The block diagram of the system, under consideration, is illustrated in Figure 5.14. The system parameters are presented in Table 5.19 [Qi, et al, 2015]. The TCSC is installed at the middle of the transmission line, rated 500kV, 60 Hz.

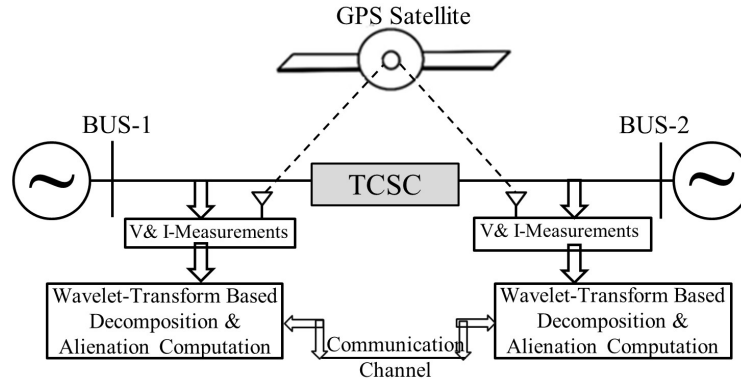


Figure 5.14: TCSC-Compensated Transmission System

5.4.2 Detection and Classification of Faults

Figure 5.15 demonstrates various steps involved in detection of AG fault. Figures 5.15 (a) and 5.15 (b) show three-phase current signals measured at bus-1 and bus-2. The respective approximate coefficients are plotted in Figures 5.15 (c) and 5.15 (d). The alienation coefficients, obtained over a quarter cycle, based on these approximate coefficients are plotted in Figures 5.15(e) and 5.15 (f). Figure 5.16 illustrates variation of fault index, computed by adding alienation coefficients of both the buses. It can also be observed that fault index of phase-A alone exceeds the threshold value, indicating AG fault.

Table 5.19 System Parameters

AC Systems at Bus-1 and Bus-2	
Positive Sequence Impedance	$Z_1 = 1.43 + j16.21\Omega$
Zero Sequence Impedance	$Z_0 = 3.068 + j28.746\Omega$
Transmission Line (300 km)	
Positive Sequence Impedance	$Z_1 = 0.0185 + j0.3766\Omega/\text{km}$
Positive Sequence Parallel Capacitive Reactance	$X_1 = 0.22789 \text{ M}\Omega\text{km}$
Zero Sequence Impedance	$Z_0 = 0.3618 + j1.2277\Omega/\text{km}$
Zero Sequence Parallel Capacitive Reactance	$X_0 = 0.34513 \text{ M}\Omega\text{km}$
TCSC	
Main Capacitor	176 μF
TCR Inductance	9.0 mH
L_d in bypass breaker circuit	0.2mH

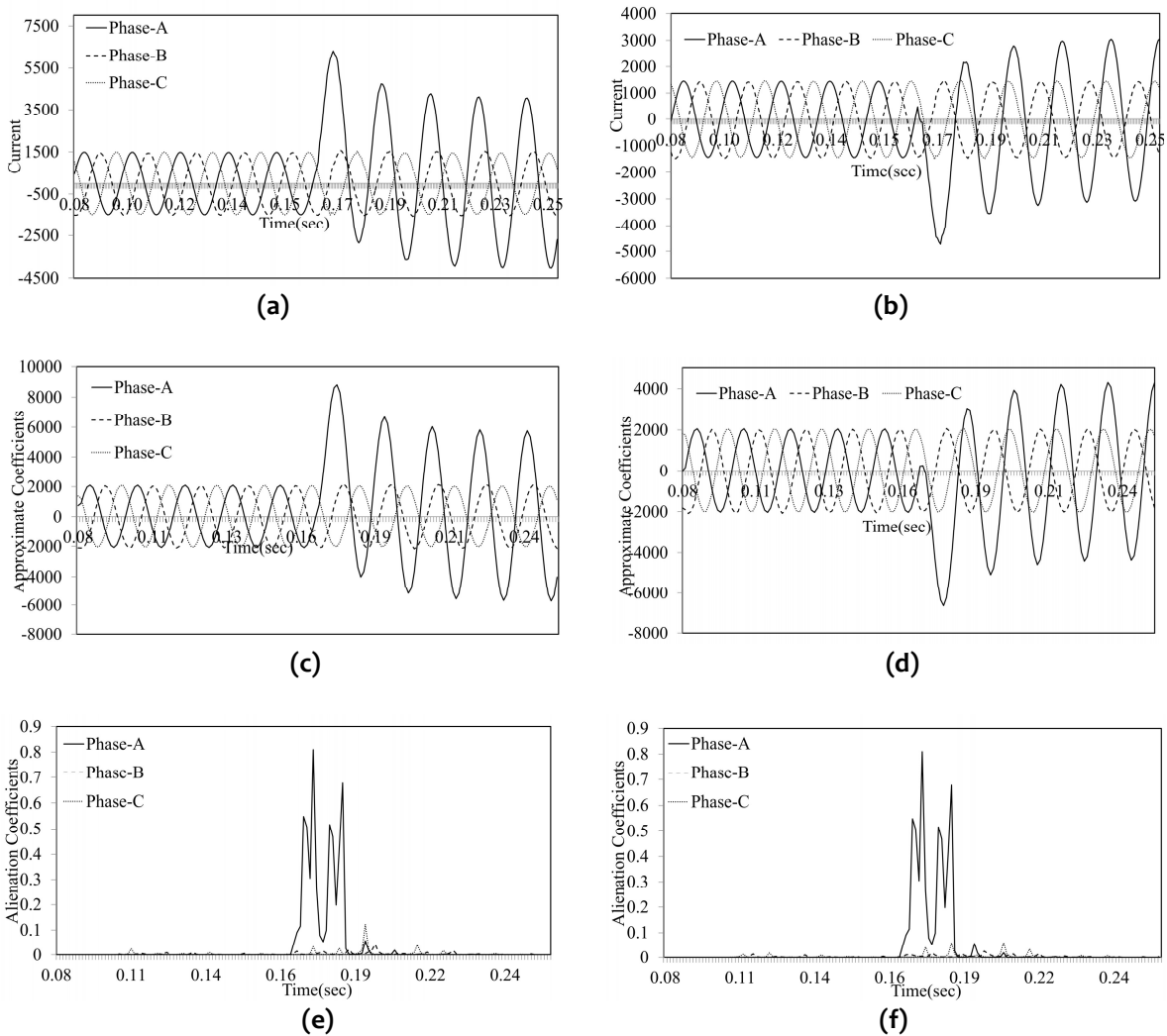


Figure 5.15: Demonstration of AG-Fault Detection: (a) Bus-1 Current Signals, (b) Bus-2 Current Signals, (c) Approximate Decomposition of Bus-1 Current Signals, (d) Approximate Decomposition of Bus-2 Current Signals, (e) Alienation Coefficients for Approximate Coefficients of Bus-1, (f) Alienation Coefficients for Approximate Coefficients of Bus-2

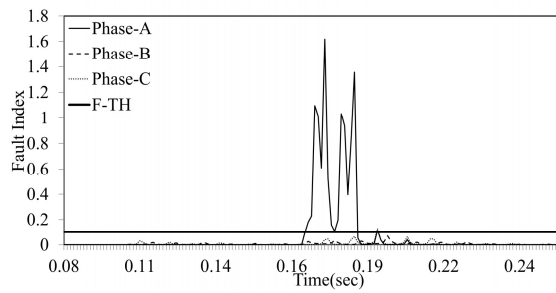


Figure 5.16: Fault Index Variation w.r.t. time for AG Fault

Figures 5.17-5.18 depict Fault Index variation of three-phases for BG, CG, AB, BC, AC, ABG, BCG, ACG and ABCG faults. Figures 5.17 (a) and 5.17 (b) show the fault index variation for BG and CG faults respectively, in which fault index of faulty phase is greater than the threshold and not for the healthy phases. Figures 5.17 (c) and 5.18 (b) depict the variation of three-phase fault indexes for AB and ABG faults respectively. From these figures, it is evident that phase-A and phase-B have fault index greater than the threshold. Similarly, Figures 5.17 (d) and 5.18 (c) illustrate the fault index variation for BC and BCG faults respectively, from which it can be observed that fault indexes of faulty phases (phase-B & C) are greater than the threshold and not for healthy phase i.e. Phase-A. The fault index variation for AC and ACG faults is shown in Figures 5.18 (a) and 5.18 (d), from these figures it is depicted that fault index for phase-A and phase-C are greater than the threshold whereas for phase-B it remains lower than the threshold, hence the faults are identified as AC and ACG fault respectively. From Figure 5.18 (e), it is evident that all the three phases have fault indexes greater than the threshold, thus it is detected and classified as ABCG fault.

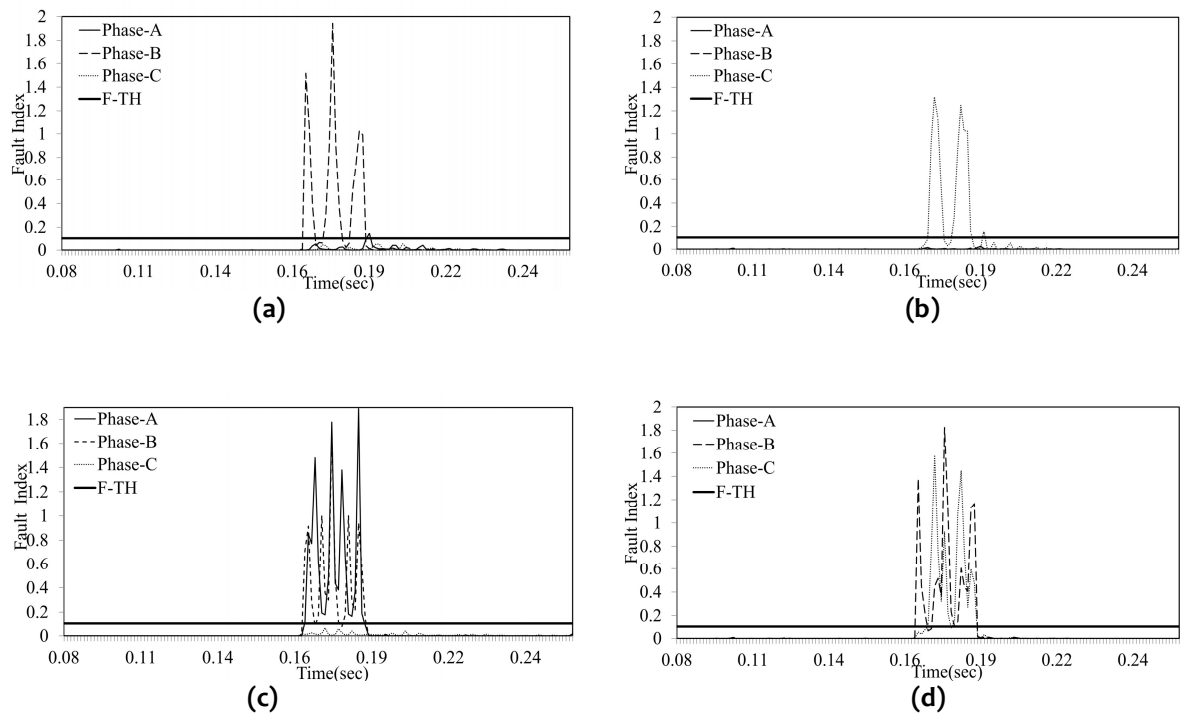


Figure 5.17: Fault Detection and Classification for: (a) BG Fault, (b) CG Fault, (c) AB Fault, (d) BC Fault

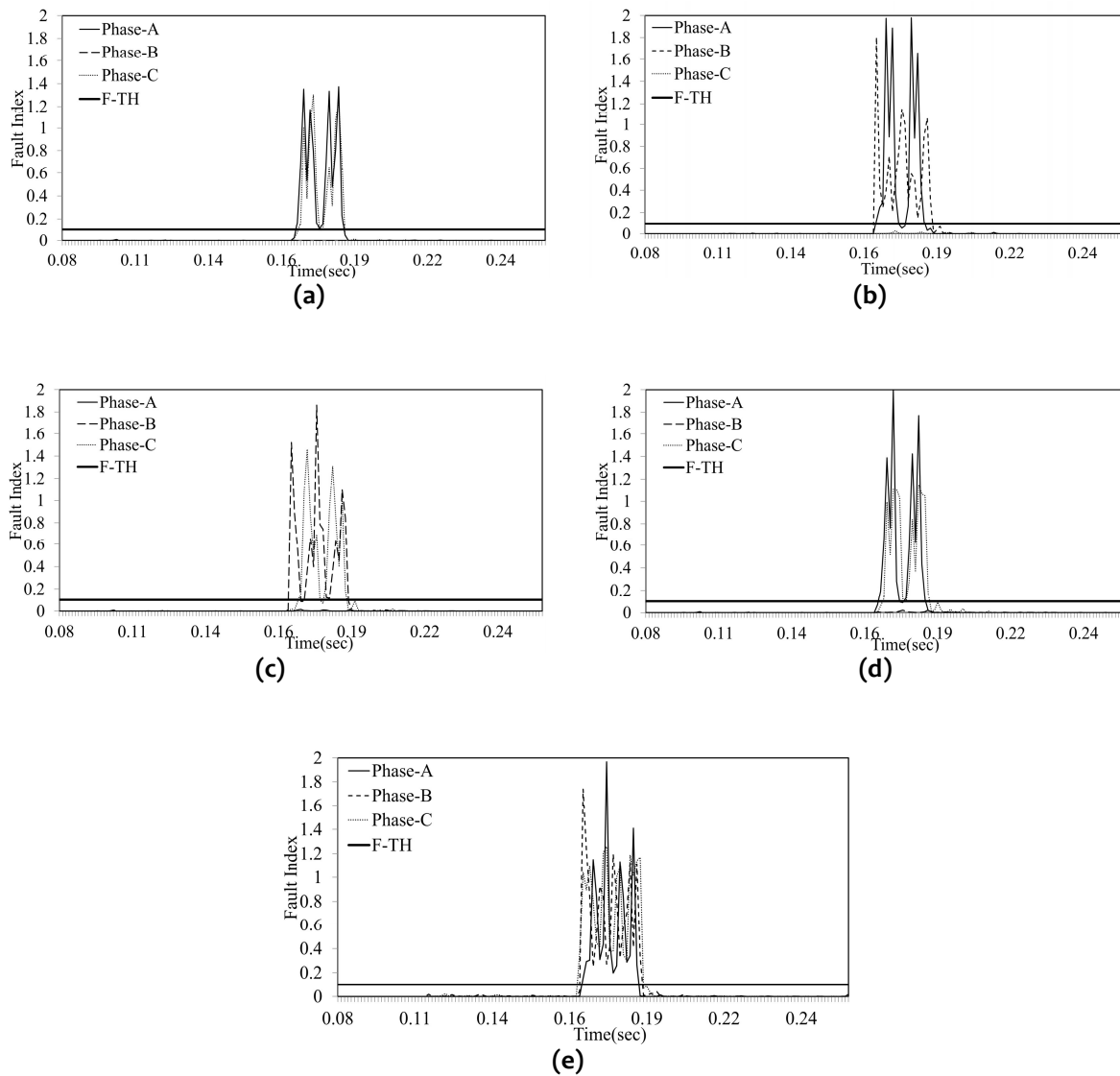


Figure 5.18: Fault Detection and Classification: (a) AC Fault, (b) ABG Fault, (c) BCG Fault, (d) ACG Fault, (e) ABCG Fault

However, the discrimination between LL and LLG faults cannot be achieved with the proposed fault index, since the fault indexes of faulty phases in both the cases show no apparent discrimination as shown in Figure 5.17(c) and 5.18(b). To discriminate LLG faults from LL faults, a ground fault index (G-FI) based on zero sequence current is computed by adding the approximate decomposition of zero sequence current over a moving window of quarter cycle. And this resultant G-FI is compared with a threshold which is termed as ground fault threshold (GF-TH=500) for discrimination purpose. Figure 5.19 depicts the G-FI variation for AB and ABG faults. It is evident from this figure that the fault with ground has G-FI greater than the threshold whereas fault without ground has a lesser value than the threshold.

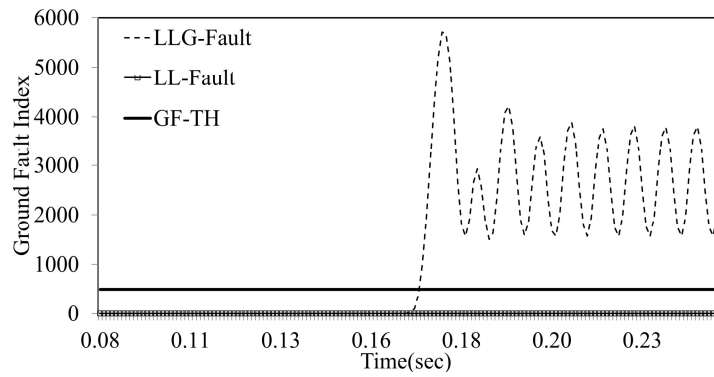


Figure 5.19: Ground Fault Index Variation

5.4.3 Case Studies

The performance of proposed algorithm has been tested for all the types of faults by varying location, incidence angle, fault impedance, TCSC location, load switching, sampling frequency and power-flow direction.

(a) Fault Location Variation

The post fault current transients are largely dependent on fault locations. Hence, there is a need to test the algorithm at various fault locations to establish its performance. For this purpose all the types of faults have been simulated for every 20 kms along the length of the line. Figure 5.20(a) illustrates variation of fault index with distance for AG fault. It is observed that fault index value of phase-A is more than the threshold and those of healthy phases (B & C) are less than the threshold. It is found that the variation of fault indexes of phases-A and B are always higher than the threshold for AB and ABG faults as shown in Figure 5.20 (b) and 5.20 (c) respectively, at all the fault locations but the fault index of phase-C remains less than the threshold. From Figure 5.20 (d), it is evident that the fault indexes of all the three phases remain greater than the threshold for ABCG fault at various locations. Thus, the proposed algorithm is not affected by variations in fault location.

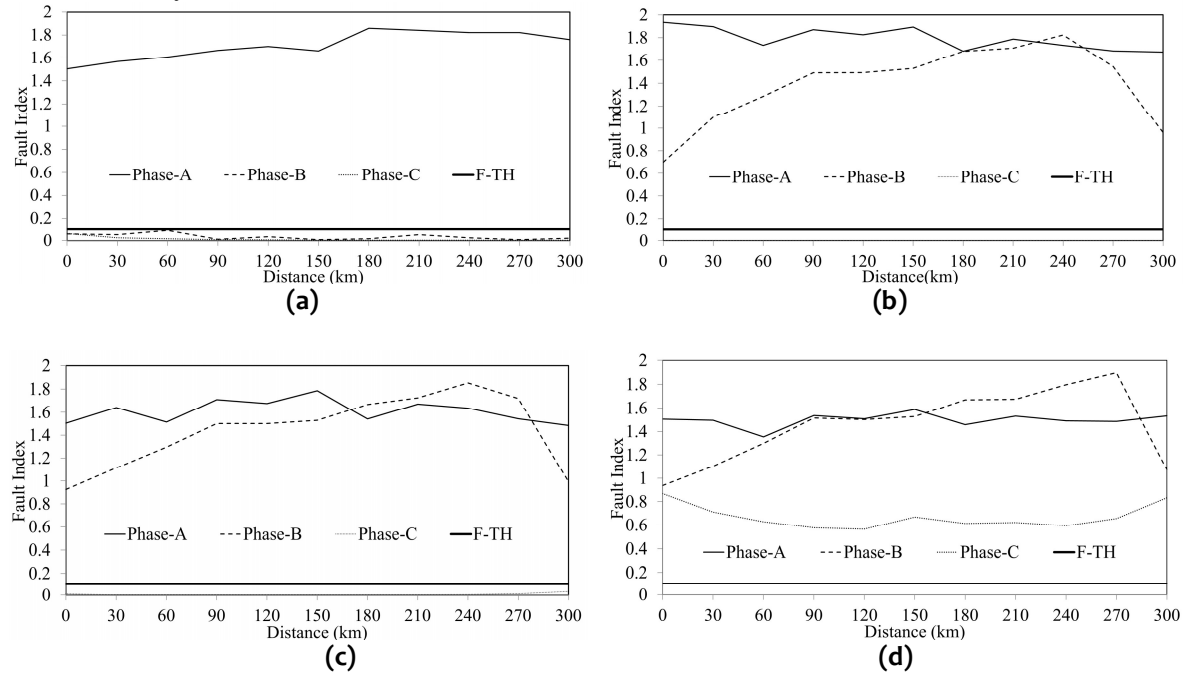


Figure 5.20: Fault Index variation for different locations: (a) AG Fault, (b) AB Fault, (c) ABG Fault, (d) ABCG Fault

(b) Effect of Fault Incidence Angle

The post fault current transients are also greatly affected by fault incipient angles. Hence, the proposed algorithm has been tested for its effectiveness with variations in fault incidence angle. The range of variation in fault incidence angle is from 0° to 180° in steps of 30° since transients obtained from 180° to 360° are found to be similar to those obtained from 0° to 180° . From Figure 5.21(a), it can be observed that the fault index of phase-A is always greater the threshold value, indicating an AG fault. However, fault indexes of other two phases remains less than the threshold. The fault index variations of phase-A and B, for AB and ABG faults, are presented in Figures 5.21 (b) and 5.21 (c). From these figure, it can be observed that fault indexes of phase-A and B are always greater than the threshold irrespective of fault incidence angle. The fault indexes of all the three phases, in case of ABCG fault, remain higher than the threshold value for different incidence angles, as illustrated in Figure 5.21 (d).

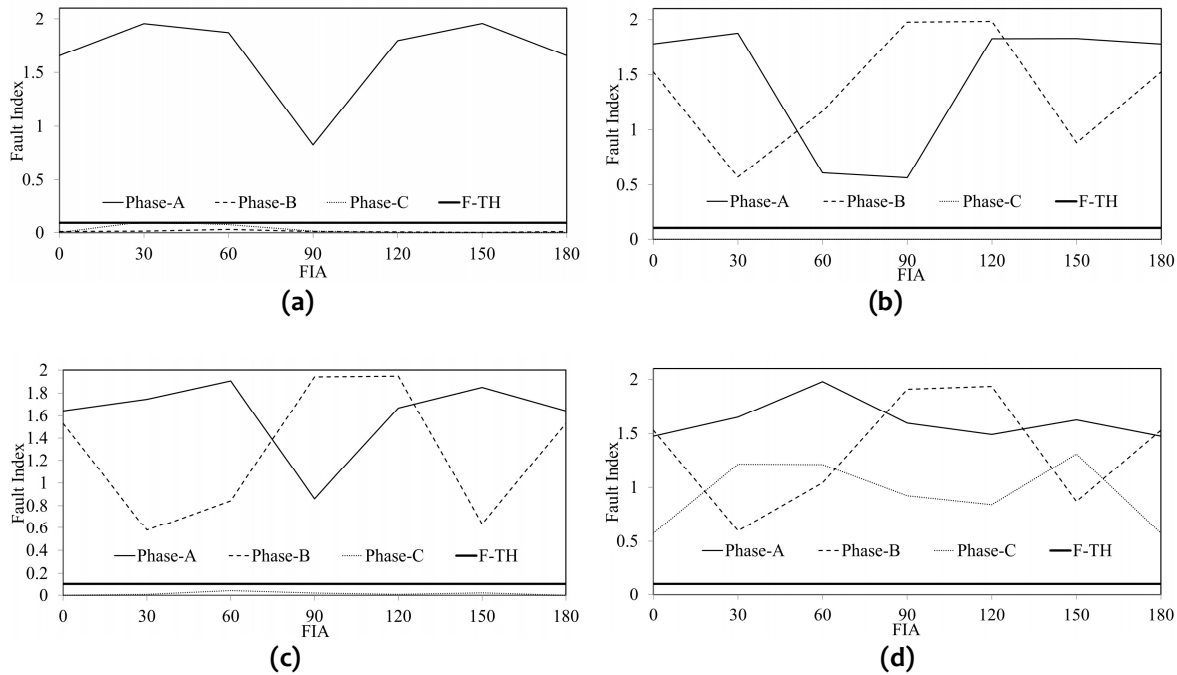


Figure 5.21: Variation of Fault Incidence Angle: (a) AG Fault, (b) AB Fault, (c) ABG Fault, (d) ABCG Fault

Tables 5.20 to 5.29 demonstrate the successful performance of proposed algorithm for all the types of faults at different locations and with variations in incidence angle.

Table 5.20: Fault Index Variation for AG Fault

FIA	0			30			60			90			120			150		
	A	B	C	A	B	C	A	B	C	A	B	C	A	B	C	A	B	C
30	1.57	0.05	0.02	1.59	0.28	0.42	1.61	0.30	0.12	1.62	0.15	0.01	1.63	0.11	0.01	1.63	0.14	0.15
60	1.61	0.09	0.02	1.63	0.06	0.23	1.68	0.04	0.14	1.65	0.06	0.03	1.69	0.03	0.00	1.70	0.03	0.01
90	1.66	0.01	0.01	1.63	0.06	0.14	1.73	0.04	0.16	1.68	0.02	0.06	1.73	0.00	0.00	1.75	0.02	0.00
120	1.70	0.03	0.01	1.67	0.03	0.07	1.77	0.06	0.07	1.75	0.02	0.04	1.78	0.00	0.00	1.78	0.02	0.00
150	1.66	0.01	0.00	1.72	0.03	0.11	1.79	0.05	0.07	1.76	0.01	0.03	1.79	0.01	0.01	1.78	0.01	0.00
180	1.86	0.02	0.00	1.67	0.01	0.05	1.87	0.02	0.07	1.87	0.08	0.05	1.85	0.01	0.01	1.82	0.01	0.00
210	1.84	0.05	0.00	1.77	0.01	0.08	1.83	0.03	0.13	1.75	0.03	0.10	1.88	0.02	0.03	1.84	0.01	0.00
240	1.82	0.02	0.00	1.73	0.01	0.11	1.71	0.03	0.12	1.89	0.33	0.08	1.82	0.10	0.03	1.85	0.01	0.02
270	1.82	0.01	0.00	1.83	0.02	0.13	1.73	0.08	0.11	1.73	0.08	0.06	1.87	0.27	0.08	1.79	0.01	0.07

Table 5.21: Fault Index Variation for BG Fault

FIA	0			30			60			90			120			150		
	A	B	C	A	B	C	A	B	C	A	B	C	A	B	C	A	B	C
30	0.02	1.06	0.01	0.02	1.15	0.01	0.00	1.98	0.07	0.02	1.99	0.03	0.01	1.92	0.02	0.01	1.96	0.05
60	0.08	1.16	0.03	0.01	1.17	0.06	0.00	1.97	0.02	0.01	1.98	0.03	0.06	1.96	0.01	0.04	1.98	0.02
90	0.04	1.32	0.05	0.01	1.19	0.03	0.00	1.96	0.01	0.00	1.97	0.03	0.03	1.96	0.01	0.02	2.00	0.02
120	0.01	1.50	0.05	0.00	1.29	0.02	0.00	1.94	0.00	0.00	1.95	0.01	0.01	1.95	0.02	0.09	1.99	0.02
150	0.06	1.52	0.05	0.04	1.29	0.03	0.00	1.94	0.01	0.00	1.93	0.00	0.01	1.95	0.07	0.05	1.99	0.01
180	0.04	1.59	0.01	0.06	1.39	0.03	0.00	1.90	0.01	0.00	1.93	0.00	0.02	1.93	0.01	0.07	2.00	0.02
210	0.03	1.65	0.07	0.01	1.67	0.09	0.00	1.89	0.06	0.00	1.91	0.01	0.01	1.92	0.00	0.02	1.98	0.01
240	0.02	1.62	0.03	0.02	1.88	0.02	0.00	1.88	0.09	0.00	1.91	0.01	0.00	1.90	0.00	0.08	1.98	0.01
270	0.09	1.37	0.04	0.05	1.05	0.03	0.02	1.84	0.01	0.00	1.90	0.01	0.01	1.88	0.00	0.02	1.98	0.03

Table 5.22: Fault Index Variation for CG Fault

FIA	0			30			60			90			120			150		
	A	B	C	A	B	C	A	B	C	A	B	C	A	B	C	A	B	C
30	0.06	0.00	1.42	0.03	0.01	1.56	0.03	0.04	1.26	0.03	0.06	1.82	0.02	0.31	0.90	0.01	0.03	0.57
60	0.02	0.00	1.41	0.01	0.01	1.47	0.02	0.08	1.28	0.02	0.04	1.74	0.10	0.14	1.07	0.01	0.06	0.81
90	0.01	0.00	1.37	0.01	0.00	1.39	0.02	0.08	1.34	0.00	0.04	1.73	0.05	0.08	0.94	0.01	0.03	0.93
120	0.02	0.00	1.31	0.00	0.00	1.36	0.01	0.05	1.33	0.01	0.01	1.75	0.02	0.03	0.81	0.06	0.03	0.88
150	0.01	0.00	1.32	0.00	0.00	1.28	0.00	0.04	1.16	0.01	0.04	1.68	0.03	0.15	0.87	0.05	0.03	1.03
180	0.00	0.01	1.21	0.00	0.00	1.26	0.00	0.01	1.24	0.01	0.01	1.66	0.06	0.03	0.99	0.10	0.08	0.86
210	0.07	0.04	1.22	0.01	0.00	1.25	0.00	0.02	1.28	0.02	0.06	1.67	0.09	0.07	1.01	0.03	0.02	0.75
240	0.06	0.05	1.11	0.00	0.00	1.30	0.00	0.03	1.24	0.01	0.03	1.63	0.01	0.02	0.86	0.01	0.03	0.64
270	0.04	0.04	1.15	0.00	0.00	1.30	0.01	0.01	1.23	0.02	0.03	1.64	0.02	0.03	0.92	0.02	0.02	0.75

Table 5.23: Fault Index Variation for AB Fault

FIA	0			30			60			90			120			150		
	A	B	C	A	B	C	A	B	C	A	B	C	A	B	C	A	B	C
30	1.90	1.10	0.00	1.94	1.98	0.00	1.96	1.95	0.00	1.96	1.96	0.00	1.95	1.95	0.00	1.93	1.91	0.00
60	1.73	1.29	0.00	1.88	1.97	0.00	1.86	1.94	0.00	1.91	1.97	0.00	1.89	1.94	0.00	1.97	1.92	0.00
90	1.87	1.49	0.00	1.83	1.93	0.00	1.89	1.96	0.00	1.87	1.98	0.00	1.88	1.94	0.00	1.81	1.93	0.00
120	1.83	1.49	0.00	1.80	2.00	0.00	1.82	1.99	0.00	1.84	1.98	0.00	1.83	1.97	0.00	1.81	1.93	0.00
150	1.89	1.53	0.00	1.80	1.96	0.00	1.81	1.97	0.00	1.82	1.98	0.00	1.82	1.98	0.00	1.83	1.94	0.00
180	1.68	1.68	0.00	1.70	1.95	0.00	1.78	1.97	0.00	1.81	1.99	0.00	1.79	1.99	0.00	1.72	1.96	0.00
210	1.79	1.71	0.00	1.80	1.96	0.00	1.87	1.99	0.00	1.81	1.99	0.00	1.81	1.99	0.00	1.86	1.99	0.00
240	1.73	1.82	0.00	1.68	1.86	0.00	1.63	1.95	0.00	1.77	1.98	0.00	1.77	2.00	0.00	1.72	2.00	0.00
270	1.68	1.54	0.00	1.68	1.99	0.00	1.69	1.99	0.00	1.76	2.00	0.00	1.70	1.99	0.00	1.73	2.00	0.00

Table 5.24: Fault Index Variation for BC Fault

FIA	0			30			60			90			120			150		
	A	B	C	A	B	C	A	B	C	A	B	C	A	B	C	A	B	C
30	0.00	1.49	1.87	0.00	1.50	1.86	0.00	1.46	1.89	0.00	1.46	1.89	0.00	1.44	1.89	0.00	1.55	1.94
60	0.00	1.56	1.92	0.00	1.51	1.86	0.00	1.54	1.92	0.00	1.87	1.91	0.00	1.36	1.67	0.00	1.56	1.98
90	0.00	1.50	1.83	0.00	1.51	1.84	0.00	1.48	1.90	0.00	1.88	1.81	0.00	1.56	1.66	0.00	1.45	1.99
120	0.00	1.52	1.91	0.00	1.53	1.87	0.00	1.49	1.81	0.00	1.85	1.78	0.00	1.41	1.83	0.00	1.48	1.99
150	0.00	1.59	1.82	0.00	1.55	1.83	0.00	1.51	1.85	0.00	1.84	1.87	0.00	1.55	1.88	0.00	1.60	1.99
180	0.00	1.57	1.82	0.00	1.57	1.85	0.00	1.53	1.83	0.00	1.73	1.82	0.00	1.48	1.84	0.00	1.54	1.99
210	0.00	1.57	1.83	0.00	1.56	1.80	0.00	1.57	1.83	0.00	1.68	1.82	0.00	1.60	1.80	0.00	1.48	1.99
240	0.00	1.77	1.85	0.00	1.55	1.87	0.00	1.62	1.76	0.00	1.62	1.83	0.00	1.32	1.75	0.00	1.60	1.98
270	0.00	1.57	1.82	0.00	1.65	1.81	0.00	1.55	1.82	0.00	1.62	1.82	0.00	1.53	1.83	0.00	1.55	1.96

Table 5.25: Fault Index Variation for AC Fault

FIA	0			30			60			90			120			150		
	A	B	C	A	B	C	A	B	C	A	B	C	A	B	C	A	B	C
30	1.89	0.00	1.42	1.98	0.00	1.51	1.98	0.00	1.34	2.00	0.00	1.67	1.28	0.00	1.12	1.28	0.00	1.12
60	1.44	0.00	1.35	1.52	0.00	1.27	1.98	0.00	1.48	1.91	0.00	1.68	1.30	0.00	1.03	1.29	0.00	1.10
90	1.29	0.00	1.41	1.48	0.00	1.33	1.38	0.00	1.17	1.50	0.00	1.78	1.31	0.00	1.15	1.32	0.00	1.05
120	1.32	0.00	1.29	1.30	0.00	1.20	1.45	0.00	1.17	1.34	0.00	1.78	1.35	0.00	1.06	1.34	0.00	1.07
150	1.33	0.00	1.30	1.33	0.00	1.33	1.35	0.00	1.33	1.33	0.00	1.77	1.37	0.00	1.11	1.35	0.00	1.09
180	1.89	0.00	1.28	1.99	0.00	1.19	1.98	0.00	1.17	1.45	0.00	1.66	1.50	0.00	1.06	1.49	0.00	1.06
210	1.95	0.00	1.27	1.99	0.00	1.27	2.00	0.00	1.13	1.65	0.00	1.63	1.13	0.00	1.10	1.22	0.00	1.02
240	1.62	0.00	1.28	1.48	0.00	1.23	1.92	0.00	1.41	1.61	0.00	1.54	1.69	0.00	0.92	1.55	0.00	1.03
270	1.49	0.00	1.23	1.52	0.00	1.23	1.59	0.00	1.25	1.71	0.00	1.63	1.63	0.00	1.07	1.67	0.00	1.03

Table 5.26: Fault Index Variation for ABG Fault

FIA	0			30			60			90			120			150		
	A	B	C	A	B	C	A	B	C	A	B	C	A	B	C	A	B	C
30	1.64	1.11	0.00	1.62	1.98	0.15	1.65	1.93	0.34	1.65	1.98	0.02	1.67	1.91	0.11	1.65	1.94	0.15
60	1.51	1.30	0.00	1.61	1.97	0.11	1.62	1.93	0.07	1.65	1.96	0.12	1.68	1.90	0.10	1.79	1.95	0.08
90	1.71	1.50	0.00	1.61	1.90	0.05	1.68	1.94	0.07	1.65	1.97	0.09	1.68	1.91	0.02	1.62	1.95	0.01
120	1.68	1.50	0.00	1.60	1.99	0.01	1.64	1.99	0.04	1.66	1.97	0.05	1.66	1.94	0.03	1.65	1.94	0.02
150	1.79	1.53	0.00	1.62	1.93	0.01	1.65	1.94	0.04	1.66	1.94	0.02	1.67	1.94	0.05	1.69	1.95	0.02
180	1.54	1.67	0.00	1.54	1.94	0.00	1.60	1.95	0.02	1.67	1.96	0.04	1.69	1.96	0.03	1.56	1.98	0.02
210	1.67	1.72	0.00	1.67	1.92	0.00	1.74	1.96	0.02	1.67	1.96	0.04	1.58	1.94	0.10	1.74	2.00	0.02
240	1.64	1.85	0.00	1.56	1.96	0.02	1.49	1.91	0.02	1.63	1.94	0.08	1.69	1.96	0.14	1.55	1.99	0.28
270	1.54	1.72	0.01	1.58	1.94	0.07	1.57	1.94	0.06	1.61	1.95	0.15	1.57	1.92	0.08	1.61	1.97	0.06

Table 5.27: Fault Index Variation for BCG Fault

FIA	0			30			60			90			120			150		
	A	B	C	A	B	C	A	B	C	A	B	C	A	B	C	A	B	C
30	0.02	0.99	0.77	0.06	1.00	1.45	0.03	1.93	1.28	0.00	1.89	1.91	0.06	1.91	1.06	0.04	1.98	0.97
60	0.08	1.21	1.44	0.04	1.03	1.41	0.02	1.93	1.37	0.00	1.92	1.86	0.02	1.75	1.03	0.04	1.99	0.92
90	0.03	1.42	1.30	0.01	1.02	1.38	0.01	1.91	1.33	0.00	1.85	1.87	0.01	1.73	1.06	0.03	1.99	1.09
120	0.07	1.50	1.41	0.01	0.87	1.42	0.00	1.83	1.35	0.01	1.82	1.84	0.01	1.87	1.18	0.01	1.98	1.10
150	0.03	1.53	1.28	0.05	0.82	1.35	0.00	1.89	1.29	0.00	1.92	1.83	0.01	1.95	1.34	0.00	1.97	1.09
180	0.01	1.62	1.42	0.08	0.70	1.42	0.01	1.86	1.38	0.00	1.86	1.72	0.06	0.03	0.99	0.00	1.98	1.08
210	0.02	1.71	1.24	0.01	0.62	1.33	0.01	1.87	1.38	0.01	1.87	1.72	0.03	1.85	0.87	0.01	1.97	1.07
240	0.01	1.83	1.58	0.02	0.61	1.32	0.01	1.85	1.27	0.02	1.88	1.69	0.08	1.81	0.96	0.03	1.95	0.98
270	0.05	1.87	1.30	0.05	0.61	1.43	0.03	1.87	1.27	0.04	1.87	1.70	0.01	1.88	1.01	0.03	1.97	0.95

Table 5.28: Fault Index Variation for ACG Fault

FIA	0			30			60			90			120			150		
	A	B	C	A	B	C	A	B	C	A	B	C	A	B	C	A	B	C
30	1.42	0.03	1.22	1.54	0.00	1.39	1.36	0.09	1.17	1.17	0.04	1.85	0.60	0.04	1.09	1.44	0.07	0.66
60	1.32	0.05	1.06	1.79	0.01	1.25	1.10	0.03	1.29	1.46	0.01	1.81	0.54	0.02	1.02	1.42	0.08	0.79
90	1.43	0.07	1.21	1.56	0.01	1.27	1.55	0.01	1.16	0.27	0.03	1.84	0.63	0.07	0.84	1.43	0.06	0.79
120	1.44	0.02	1.13	1.83	0.00	1.07	1.44	0.00	1.11	0.52	0.01	1.81	0.56	0.04	0.97	1.43	0.04	0.96
150	1.43	0.01	1.12	1.83	0.01	1.27	1.89	0.00	1.09	0.57	0.00	1.83	0.73	0.02	1.14	1.46	0.03	1.02
180	1.50	0.02	1.12	1.86	0.00	1.09	2.00	0.01	1.08	0.68	0.01	1.69	0.41	0.02	1.09	1.56	0.04	0.99
210	1.55	0.01	1.11	1.48	0.01	1.18	2.00	0.02	1.05	0.71	0.02	1.66	0.53	0.02	1.01	1.37	0.01	0.98
240	1.55	0.08	1.16	1.48	0.02	1.13	1.94	0.10	1.28	0.52	0.01	1.56	0.53	0.05	1.01	1.40	0.01	1.01
270	1.68	0.04	1.15	1.56	0.02	1.08	1.91	0.04	1.17	0.54	0.09	1.65	0.96	0.08	0.98	1.70	0.01	0.92

Table 5.29: Fault Index Variation for ABCG Fault

FIA	0			30			60			90			120			150		
	A	B	C	A	B	C	A	B	C	A	B	C	A	B	C	A	B	C
30	1.50	1.10	0.71	1.93	1.92	1.33	1.98	1.91	1.24	1.51	1.91	1.91	1.51	1.91	1.24	1.50	1.95	1.27
60	1.35	1.30	0.63	1.67	1.94	1.29	1.99	1.91	1.33	1.56	1.92	1.85	1.50	1.82	1.15	1.57	1.96	1.28
90	1.54	1.51	0.58	1.98	1.86	1.29	1.99	1.91	1.23	1.47	1.90	1.86	1.50	1.80	1.31	1.47	1.95	1.21
120	1.51	1.50	0.56	1.76	1.95	1.22	2.00	1.92	1.15	1.49	1.89	1.83	1.50	1.90	1.23	1.49	1.94	1.24
150	1.59	1.53	0.67	1.65	1.88	1.24	1.98	1.90	1.27	1.48	1.91	1.83	1.50	1.92	1.39	1.50	1.95	1.31
180	1.46	1.67	0.61	1.64	1.90	1.24	1.86	1.91	1.18	1.53	1.91	1.71	1.54	1.91	1.30	1.49	1.96	1.27
210	1.53	1.67	0.62	1.88	1.88	1.24	1.96	1.91	1.21	1.61	1.91	1.69	1.34	1.91	1.31	1.48	1.99	1.22
240	1.49	1.80	0.59	1.46	1.93	1.23	1.77	1.88	1.29	1.57	1.90	1.61	1.57	1.89	1.09	1.35	1.93	1.36
270	1.49	1.90	0.66	1.48	1.90	1.26	1.96	1.91	1.24	1.56	1.91	1.68	1.50	1.91	1.26	1.51	1.97	1.26

(c) Variation of Fault Impedance

Faults with high impedances are difficult to detect due to low level of post-fault currents owing to low sensitivity of the relay. The sensitivity of the proposed protection scheme has been

established by selecting the fault impedances from 0-100Ω under this case study. Figure 5.22 illustrates the fault index variation of all the three-phases for different types of faults, for a fault impedance of 20Ω. Figure 5.22 (a) depicts that for phase-A (faulty phase) fault index is greater than the threshold and not for phase-B and phase-C (healthy phase), hence detects the fault as phase to ground (AG) fault. Figures 5.22 (b) and 5.22 (c) show the fault index variation for BG and CG faults respectively, in which fault index of faulty phase is greater than the threshold and not for the healthy phases. Figures 5.22 (d) and 5.23 (a) depict the variation of three-phase fault indexes for AB and ABG faults respectively. Form these figures, it is evident that phase-A and phase-B have fault index greater than the threshold. Similarly, Figures 5.22 (e) and 5.23 (b) illustrate the fault index variation for BC and BCG faults respectively, from which it can be observed that fault indexes of faulty phases (phase-B & C) are greater than the threshold and not for healthy phase i.e. Phase-A. The fault index variation for AC and ACG faults is shown in Figures 5.22 (f) and 5.23 (c), from these figures it is depicted that fault index for phase-A and phase-C are greater than the threshold whereas for phase-B it remains lower than the threshold, hence faults are identified as AC and ACG fault respectively. Figure 5.23 (d) shows that for all the three phases, fault index is greater than the threshold, hence it is detected as three phase to ground (ABCG) fault. Thus, it is evident that the fault impedance has no effect on proposed algorithm. Thus, it is evident that the fault impedance has no effect on proposed algorithm.

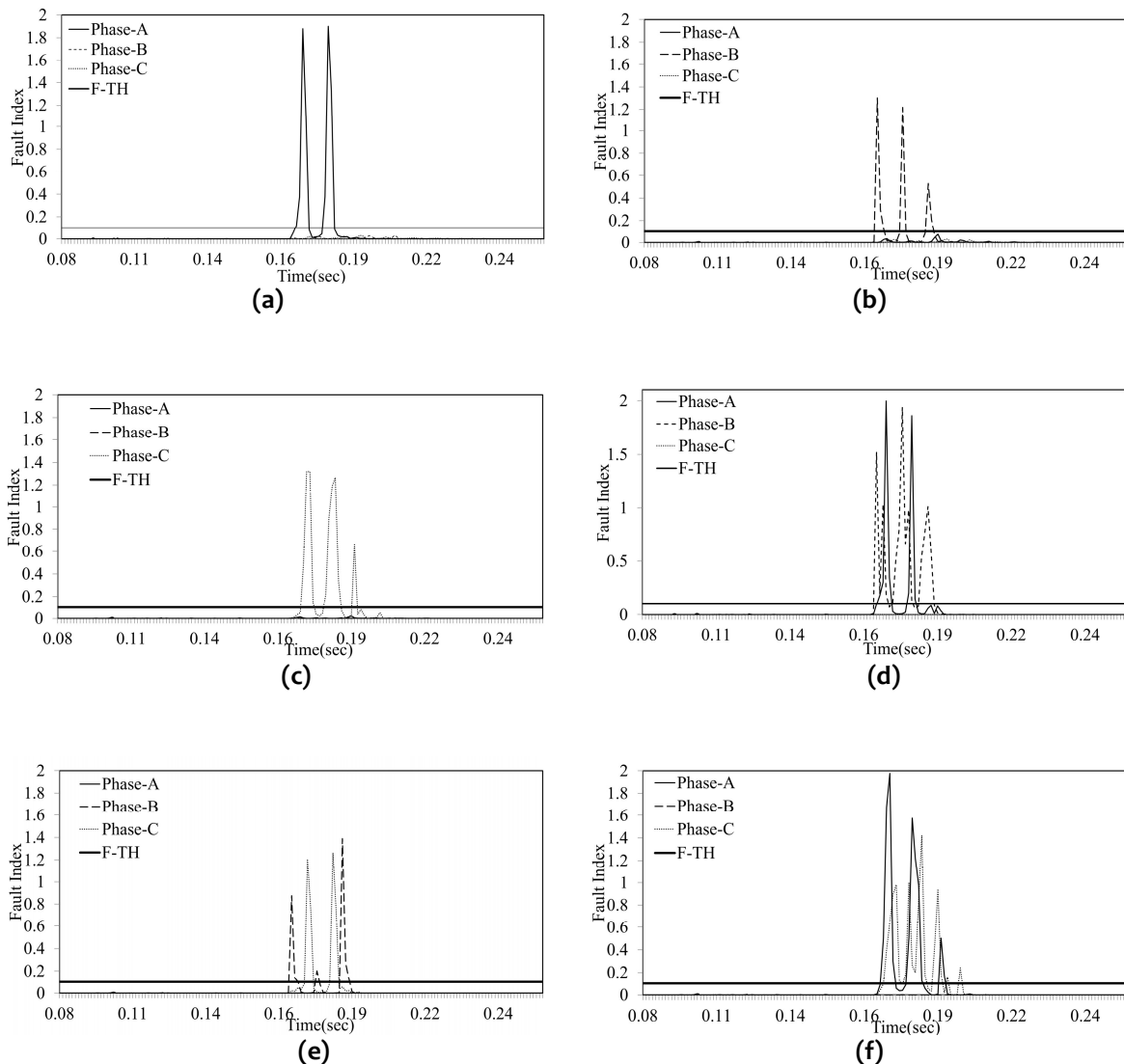


Figure 5.22: Fault Index Variation for high impedance faults: (a) AG Fault, (b) BG Fault, (c) CG Fault, (d) AB Fault, (e) BC Fault, (f) AC Fault

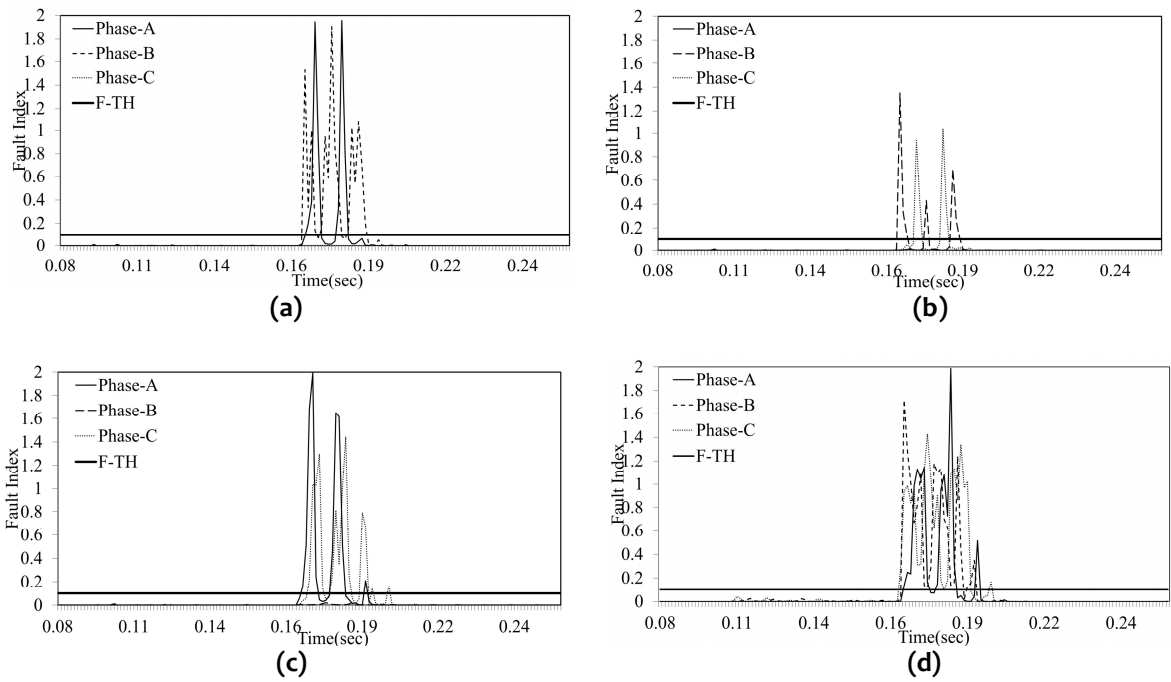


Figure 5.23: Fault Index Variation for high impedance faults: (a) ABG Fault, (b) BCG Fault, (c) ACG Fault, (d) ABCG Fault

(d) Effect of TCSC Location

The location of TCSC affects the magnitude and transients of bus-currents. Hence, the performance of the proposed algorithm is verified by changing the TCSC location to receiving end (Bus-2). Figures 5.24 (a-d) illustrate the variation of three-phase fault index for AG, AB, ABG and ABCG faults respectively. From these figures, it can be observed that the fault index of faulty phases alone, exceed the threshold value. Hence, it is established that the location of TCSC does not affect the performance of the proposed algorithm.

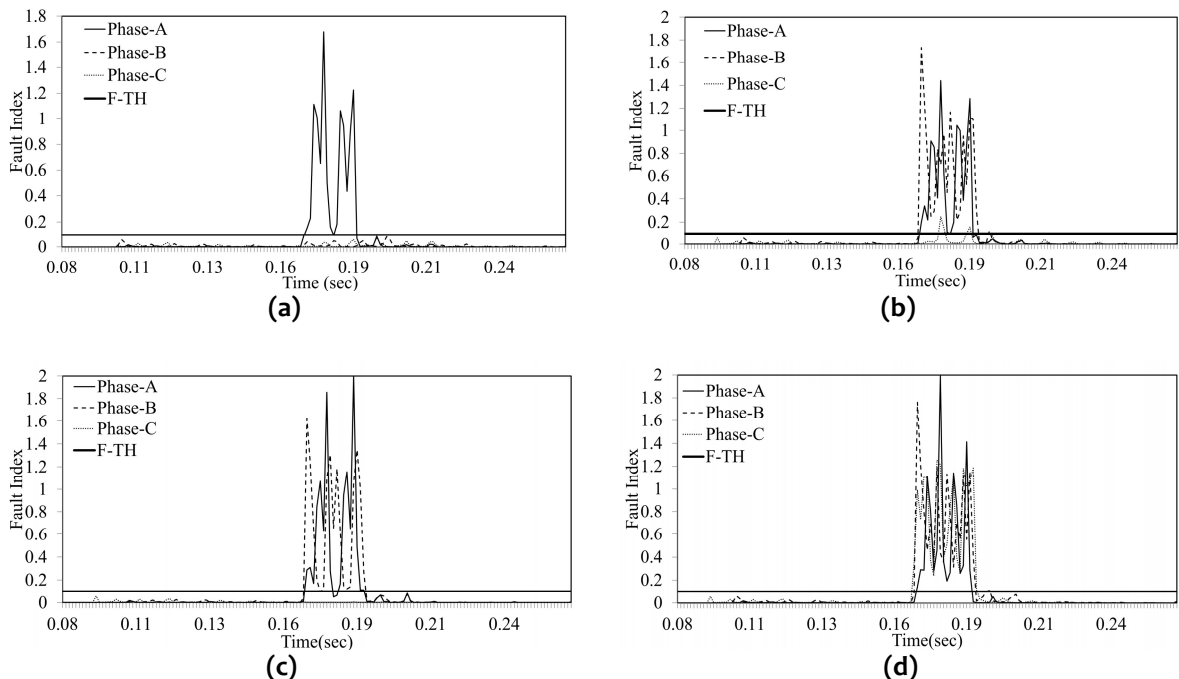


Figure 5.24: Fault Index Variation for TCSC installed at receiving end: (a) AG Fault, (b) AB Fault, (c) ABG Fault, (d) ABCG Fault

(e) Performance in Noisy Environment

The current signals are contaminated with noise to prove the robustness of the proposed scheme to detect and classify the faults in the noisy environment. For this purpose the levels of SNRs considered, is 40dB-10dB. Figure 5.25 depicts variation of three-phase fault index for different types of faults, with 10dB white Gaussian noise. Figure 5.25(a) depicts variation of fault index for AG fault. The fault index of phase-A is greater than the threshold and that of other phases is less than the threshold, thus illustrating AG fault. Figure 5.25(b) and 5.25(c) illustrate that for phase-A and phase-B, fault index is greater than the threshold and not for phase-C, and hence the faults are detected as AB and ABG faults respectively. Figure 5.25(d) shows that for all the three phases, fault index is greater than the threshold. Hence it is detected as ABCG fault. Thus, it is proved that the proposed algorithm can detect and classify the faults even in the noisy environment.

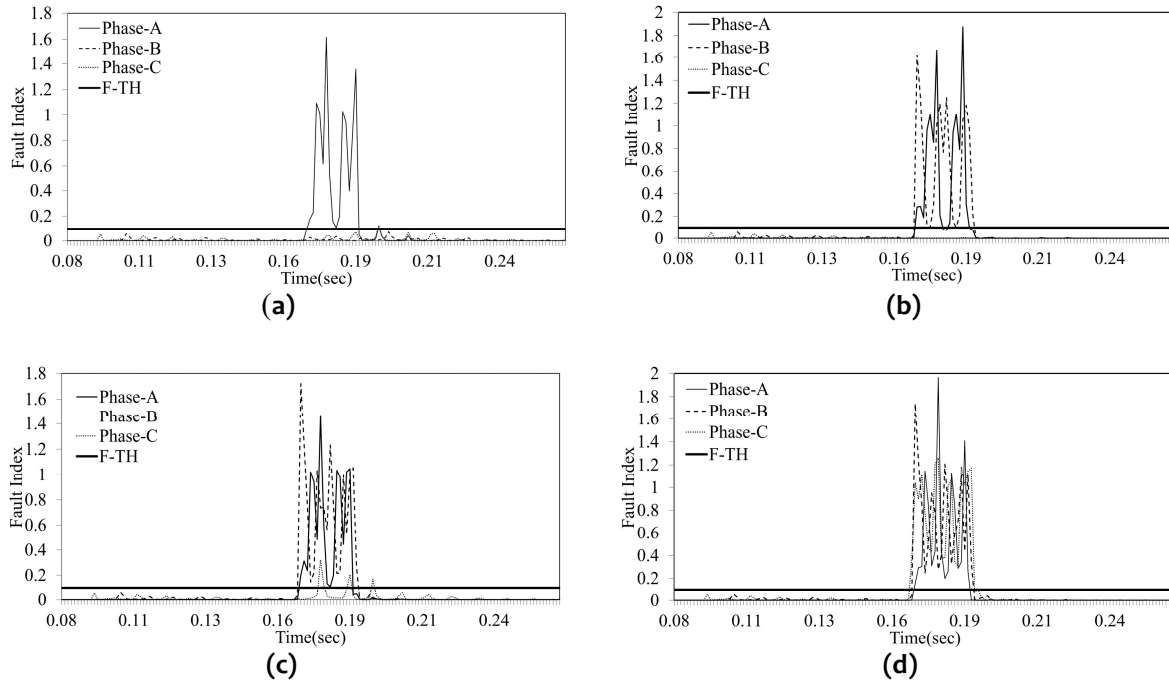


Figure 5.25: Fault Index Variation in Noisy Environment: (a) AG Fault, (b) AB Fault, (c) ABG Fault, (d) ABCG Fault

(f) Effect of Loading

Switching of loads also causes transients in current signals which may affect the performance of proposed protection algorithm, which works on the on basis of current signals. Hence, the performance of the proposed algorithm has been evaluated for 10% and 20 % of load changes. The highest fault indexes associated with the load switching is found to be 0.07 which is very low as compared to threshold (0.10) value. Thus, it is evident that the proposed algorithm has not been affected by load switching.

(g) Effect of Power-Flow Direction

To consider the effect of power-flow direction in the proposed algorithm, it has been tested on reverse power flow condition. Since the proposed scheme is making use of data from both the buses, the obtained results corresponding to reverse power-flow are found to be same as in case of original power flow.

(h) Effect of Sampling Frequency

The algorithm has been tested with sampling frequency of 0.96 kHz, 1.92 kHz, 3.84 kHz and 7.68 kHz; it has been observed that increase in frequency has no considerable improvement

in terms of accuracy and speed of proposed protection scheme. However the reduction in sampling frequency increases the detection time.

5.4.4 Location of Fault

Estimation of fault location has been carried out, followed by fault detection and classification, using Artificial Neural Network. A multi-layer feed-forward neural network, whose structure is shown in Figure 5.26, is used to locate the fault. The details related to structure of ANN are presented in Table 5.30.

Table 5.30: Structure of ANN

S. No.	Name of Layers	No. of Neurons	Transfer Function
1	Input Layer	48	Purelin
2	Hidden-Layer-1	15	Log-Sigmoid
3	Hidden- Layer-2	9	Log-Sigmoid
4	Output Layer	1	Purelin

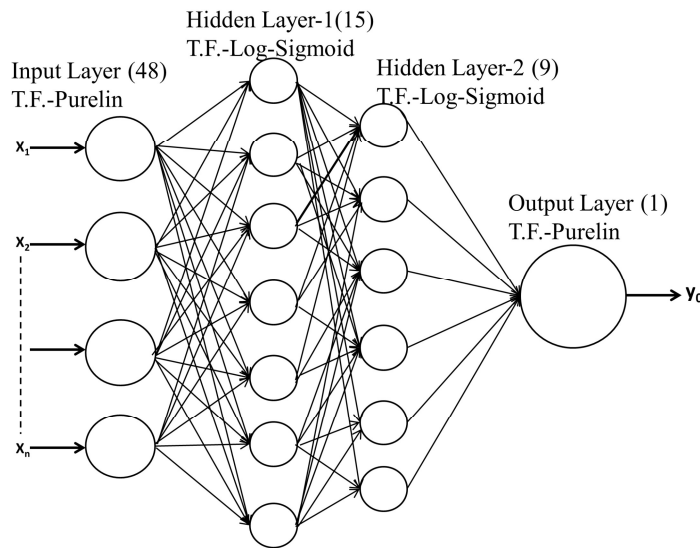


Figure 5.26: ANN Structure

The input to neural network is 48 approximate coefficients, of each phase voltage and current signal, obtained over a quarter cycle, from both the ends of the line. Thus, the total number of inputs is $[2(\text{buses}) * \{3(\text{phase voltage}) + 3(\text{phase current})\}] * 4$ coefficients.

The output of the ANN will be fault location (in kms) from bus-1. The training of proposed ANN has been carried out by feeding 48 approximate coefficients of post-fault three-phase voltage and current signals, obtained over a quarter cycle. The trained ANN has been tested for its performance with the data obtained by data obtained from simulating all the types of faults at new locations. The percentage error in fault location is calculated as:-

$$\%Error = \frac{|NNDistance - ActualDistance|}{L} * 100$$

Tables 5.31 (a-b) demonstrates the accuracy using proposed ANN. From which, it can be observed that the maximum and average error, in locating the faults, is 1.97% and 0.81% respectively.

Table 5.31 (a): Estimation of Fault Location for AG, BG, CG, AB and BC faults

S.No	Fault-type	Actual Location	ANN Location	% Error
1	Phase-A to G	21	25.35	1.45
2	Phase-A to G	93	95.86	0.95
3	Phase-A to G	169	169.50	0.17
4	Phase-A to G	217	216.46	0.18
5	Phase-A to G	275	276.24	0.41
6	Phase-B to G	21	26.92	1.97
7	Phase-B to G	93	90.09	0.97
8	Phase-B to G	169	166.17	0.94
9	Phase-B to G	217	217.06	0.02
10	Phase-B to G	275	280.61	1.87
11	Phase-C to G	21	21.16	0.05
12	Phase-C to G	93	90.70	0.77
13	Phase-C to G	169	168.08	0.31
14	Phase-C to G	217	214.25	0.92
15	Phase-C to G	275	278.73	1.24
16	Phase-A to B	21	25.09	1.36
17	Phase-A to B	93	97.42	1.47
18	Phase-A to B	169	169.91	0.30
19	Phase-A to B	217	219.25	0.75
20	Phase-A to B	275	279.05	1.35
21	Phase-B to C	21	21.05	0.02
22	Phase-B to C	93	91.21	0.60
23	Phase-B to C	169	168.63	0.12
24	Phase-B to C	217	211.73	1.76
25	Phase-B to C	275	270.87	1.38

5.4.5 Performance in Absence of TCSC

In this section, efforts have been made to prove the ability of algorithm to detect and classify the faults, even in the absence of TCSC (due to maintenance or outage). For this purpose, TCSC has been disconnected from the transmission line and various types of faults have been simulated. Table 5.32 compares the performance of proposed protection scheme with and without TCSC. From this table, it can be observed that the fault indexes of faulty phases remains higher than the threshold, both in presence and absence of TCSC. Thus, it is evident that the proposed algorithm is not affected by presence or absence of TCSC.

Table 5.31 (b): Estimation of Fault Location for AC, ABG, BCG, ACG and ABCG faults

S.No	Fault-type	Actual Location	ANN Location	% Error
1	Phase-A to C	21	19.89	0.37
2	Phase-A to C	93	94.25	0.42
3	Phase-A to C	169	169.35	0.12
4	Phase-A to C	217	216.76	0.08
5	Phase-A to C	275	274.28	0.24
6	Phases-AB to G	21	23.03	0.68
7	Phases-AB to G	93	92.52	0.16
8	Phases-AB to G	169	165.09	1.30
9	Phases-AB to G	217	215.97	0.34
10	Phases-AB to G	275	269.90	1.70
11	Phases-BC to G	21	23.39	0.80
12	Phases-BC to G	93	98.52	1.84
13	Phases-BC to G	169	171.27	0.76
14	Phases-BC to G	217	213.89	1.04
15	Phases-BC to G	275	280.09	1.70
16	Phases-AC to G	21	20.07	0.31
17	Phases-AC to G	93	98.13	1.71
18	Phases-AC to G	169	166.12	0.96
19	Phases-AC to G	217	217.84	0.28
20	Phases-AC to G	275	271.69	1.10
21	Phases-ABC to G	21	19.51	0.50
22	Phases-ABC to G	93	94.29	0.43
23	Phases-ABC to G	169	170.68	0.56
24	Phases-ABC to G	217	212.83	1.39
25	Phases-ABC to G	275	275.98	0.33

Table 5.32: Performance Comparison

S. No.	Fault Type	Phase-A		Phase-B		Phase-C	
		Without TCSC	With TCSC	Without TCSC	With TCSC	Without TCSC	With TCSC
1	AG	1.65	1.65	0.01	0.01	0.00	0.00
2	BG	0.06	0.05	1.51	1.52	0.00	0.00
3	CG	0.01	0.01	0.01	0.00	0.87	0.86
4	AB	1.78	1.78	1.52	1.52	0.00	0.00
5	BC	0.00	0.00	1.37	1.38	0.90	0.99
6	AC	1.35	1.35	0.01	0.00	1.00	1.00
7	ABG	1.64	1.64	1.52	1.53	0.01	0.00
8	BCG	0.02	0.01	1.51	1.52	0.76	0.76
9	ACG	1.39	1.39	0.00	0.01	1.00	0.99
10	ABC	1.47	1.47	1.52	1.53	0.58	0.58

5.5 UPFC-COMPENSATED TRANSMISSION SYSTEM

5.5.1 System Model and Parameters

The block diagram of the power system and the proposed algorithm is illustrated in Figure 5.27. Various parameters of power system, under consideration, are presented in Table 5.33 [Moravej, Pazoki and Khederzadeh, 2014]. The UPFC is installed at the middle of the transmission line, rated 500kV, 60 Hz.

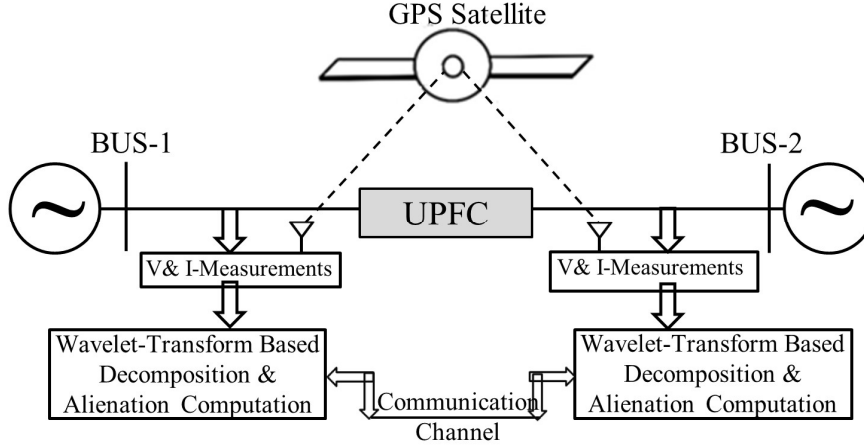


Figure 5.27: UPFC-Compensated Transmission System

Table 5.33: SYSTEM PARAMETERS

AC Sources (500 kV)	
Bus-1 & Bus-2 Source Impedance	$Z_s = 2.9142 + j29.4117 \Omega$
Transmission Line (300 km)	
Resistance	$R_o = 0.3864 \Omega/\text{km}$ $R_i = 0.0254 \Omega/\text{km}$
Inductance	$L_o = 4.1264 \times 10^{-3} \text{ H}/\text{km}$ $L_i = 9.337 \times 10^{-4} \text{ H}/\text{km}$
Capacitance	$C_o = 7.751 \times 10^{-9} \text{ F}/\text{km}$ $C_i = 12.74 \times 10^{-9} \text{ F}/\text{km}$
UPFC	
Shunt Converter:	
Nominal Power	100MVA
Coupling Transformer Voltage	500/15 kV
Series Converter:	
Nominal Power	100MVA
Voltage Injection	50 kV (10%)
Coupling Transformer Voltage	12.5/12.5 kV

5.5.2 Simulation Results

Figure 5.28 demonstrates various steps involved in detection of AG fault. Figures 5.28 (a) and 5.28 (b) show three-phase current signals measured at bus-1 and bus-2. The respective approximate coefficients are plotted in Figures 5.28 (c) and 5.28 (d). The alienation coefficients, obtained over a quarter cycle, based on these approximate coefficients are plotted in Figures 5.28 (e) and 5.28 (f). Figure 5.28(g) illustrates variation of fault index, computed by adding alienation coefficients of both the buses. It can also be observed that fault index of phase-A alone exceeds the threshold value, indicating AG fault.

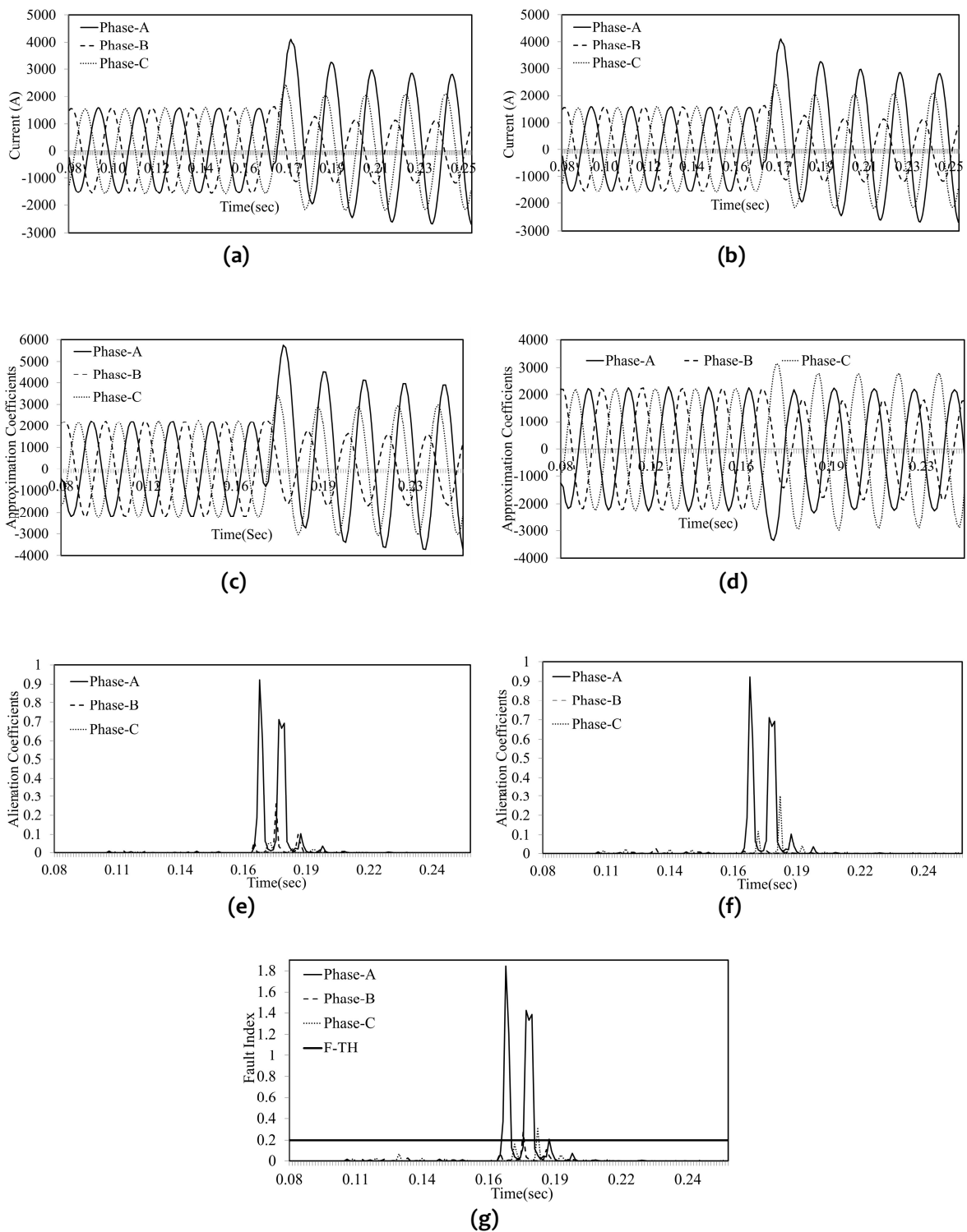


Figure 5.28: Demonstration of AG-Fault Detection: (a) Bus-1 Current Signals, (b) Bus-2 Current Signals, (c) Approximate Decomposition of Bus-1 Current Signals, (d) Approximate Decomposition of Bus-2 Current Signals, (e) Alienation Coeff. for App. Coeff. of Bus-1, (f) Alienation Coeff. for App. Coeff. of Bus-2, (g) Fault Index Variation

Figure 5.29 depicts Fault Index variation of three-phases for AB, ABG and ABCG faults. From Figure 5.29 (a) and Figure 5.29 (b), it is evident that the fault indexes of phase-A and B are higher than threshold and hence it is detected as phase to phase fault. It can be observed from Figure 5.29(c) that all the three-phases have fault index greater than the threshold. Thus, it is classified as three-phase fault.

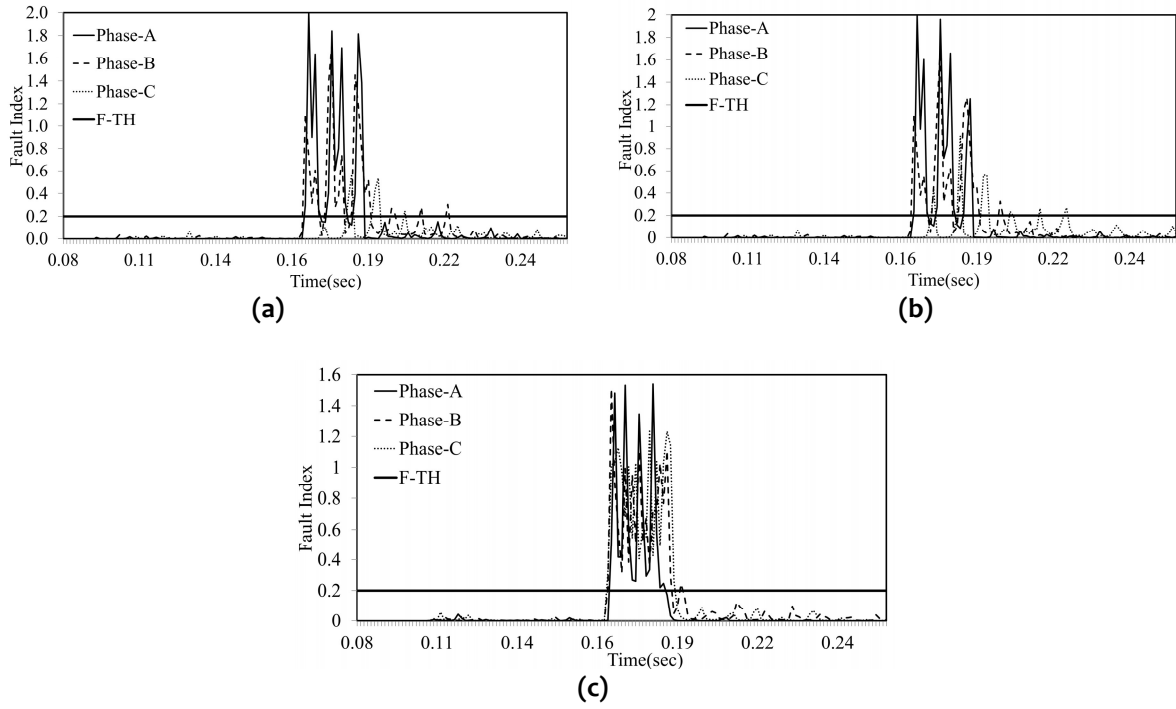


Figure 5.29: Fault Detection and Classification: (a) AB Fault, (b) ABG Fault, (c) ABCG Fault

However, the discrimination between LL and LLG faults cannot be achieved with the proposed fault index, since the fault indexes of faulty phases in both the cases show no apparent discrimination as shown in Figures 5.29 (a) and 5.29 (b). To discriminate LLG faults from LL faults, a ground fault index (G-FI) based on zero sequence current is computed by adding the approximate decomposition of zero sequence current over a moving window of quarter cycle. And this resultant G-FI is compared with a threshold which is termed as ground fault threshold (GF-TH) for discrimination purpose. Figure 5.30 depicts the G-FI variation for AB and ABG faults. It is evident from this figure that the fault with ground has G-FI greater than the threshold whereas fault without ground has a lesser value than the threshold.

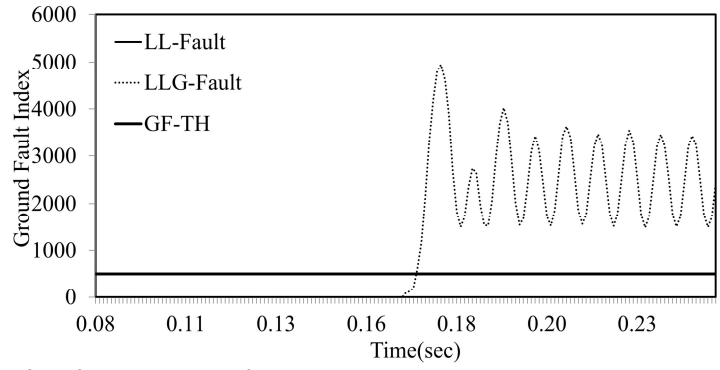


Figure 5.30: Ground Fault Index variation with time

5.5.3 Case Studies

The performance of proposed algorithm has been tested for all the types of faults by varying fault location, incidence angles, impedance of faults, for noise contamination and load switching.

(a) Fault Location Variation

The post fault current transients are largely dependent on fault locations. Hence, there is a need to test the algorithm at various fault locations to establish its performance. For this purpose all the types of faults have been simulated for every 20 kms along the length of the line. Figure 5.31(a) illustrates variation of fault index with distance for AG fault. It is observed that fault index value of phase-A is more than the threshold and those of healthy phases (B & C) are less than the threshold. It is found that the variation of fault indexes of phases-A and B are always higher than the threshold for AB and ABG faults as shown in Figure 5.31(b) and 5.31(c) respectively, at all the fault locations but the fault index of phase-C remains less than the threshold. From Figure 5.31(d), it is evident that fault indexes of all the three phases remain greater than the threshold for ABCG fault at various locations. Thus, the proposed algorithm is not affected by variations in fault location.

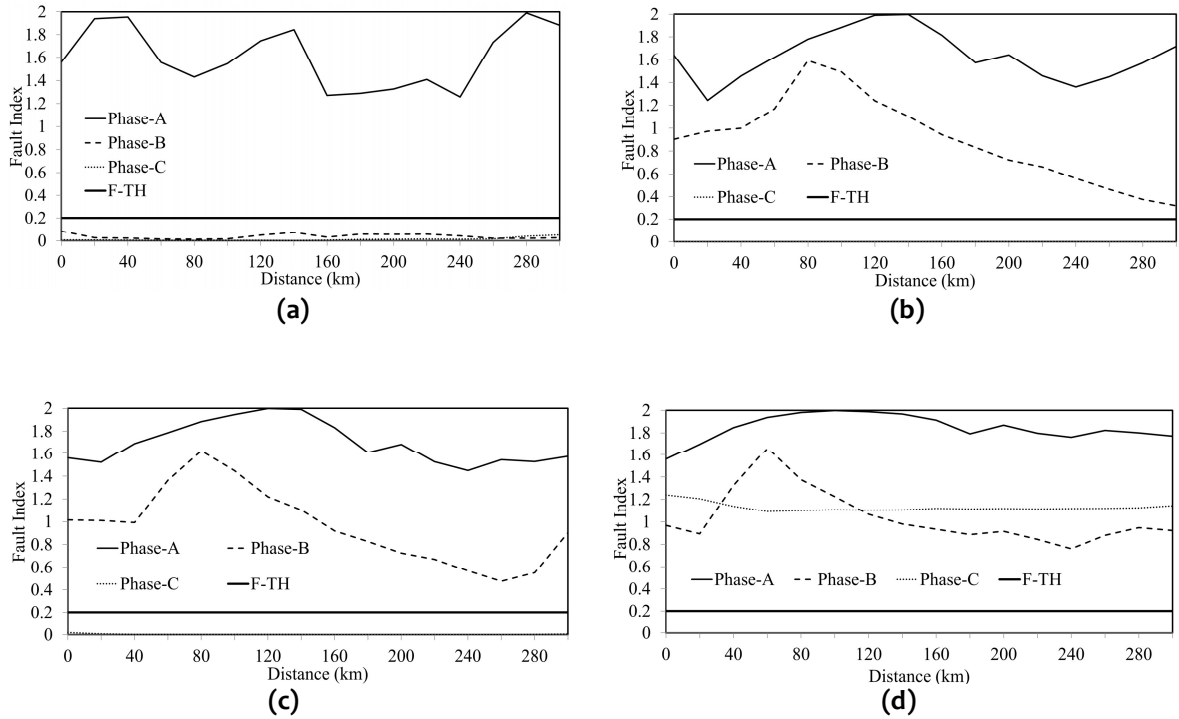


Figure 5.31: Fault Index variation for different locations: (a) AG Fault, (b) AB Fault, (c) ABG Fault, (d) ABCG Fault

(b) Fault Incidence Angle Variation

The post fault current transients are also greatly affected by fault incidence angles. Hence, the proposed algorithm has been tested for its robustness with variations in fault incidence angle. The range of variations of fault incidence angle considered from 0° to 180° in steps of 30° since transients obtained from 180° to 360° are found to be similar to those obtained from 0° to 180° . From Figure 5.32 (a), it can be observed that the fault index of phase-A is always greater than the threshold value and those of other two phase remains less than the threshold, indicating AG fault. The fault index variations of phase-A and B, for AB and ABG faults, are presented in Figures 5.32 (b) and 5.32 (c). From these figure, it can be observed that fault indexes of phase-A and B are always greater than the threshold irrespective of fault incidence angle. The fault indexes of all the three phases, in case of ABCG fault, remain higher than the threshold value for different incidence angles, as illustrated in Figure 5.32 (d).

Tables 5.34 - 5.43 demonstrates the successful performance of proposed algorithm for BG, BCG, CG and ACG faults at different locations and with variations in incidence angle.

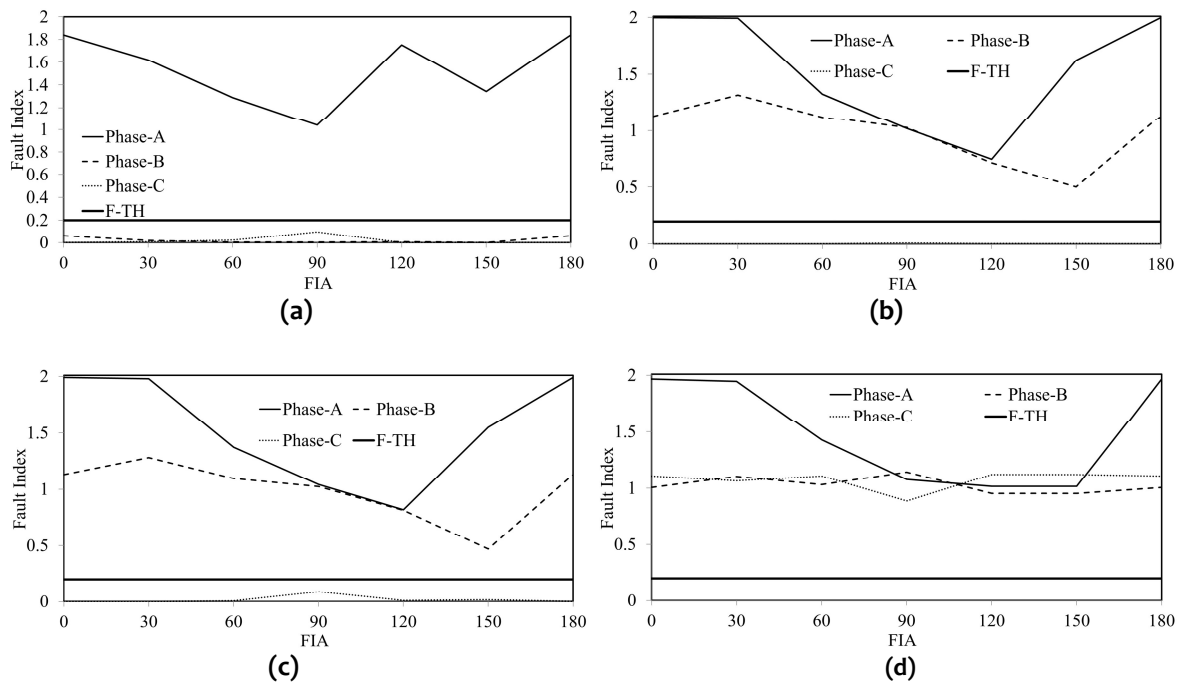


Figure 5.32: Variation of Fault Incidence Angle: (a) AG Fault, (b) AB Fault, (c) ABG Fault, (d) ABCG Fault

Table 5.34: Fault Index Variation with different locations and fault incidence angles for AG Fault

FIA	0			30			60			90			120			150		
	A	B	C	A	B	C	A	B	C	A	B	C	A	B	C	A	B	C
30	1.27	0.04	0.03	1.09	0.04	0.07	1.15	0.06	0.04	1.56	0.05	0.05	1.59	0.04	0.07	1.55	0.06	0.16
60	1.75	0.03	0.08	1.35	0.03	0.07	1.98	0.03	0.07	1.96	0.09	0.10	1.98	0.03	0.13	1.97	0.03	0.12
90	1.99	0.03	0.03	1.98	0.02	0.04	1.41	0.02	0.07	1.88	0.19	0.07	1.84	0.22	0.06	1.88	0.16	0.03
120	1.82	0.02	0.05	1.77	0.01	0.04	1.79	0.02	0.06	1.47	0.15	0.06	1.49	0.15	0.06	1.49	0.15	0.06
150	1.65	0.02	0.05	1.69	0.01	0.05	1.99	0.01	0.05	1.53	0.17	0.10	1.55	0.14	0.07	1.60	0.10	0.06
180	1.52	0.14	0.17	1.46	0.20	0.12	1.59	0.08	0.13	1.49	0.02	0.02	1.37	0.14	0.10	1.30	0.07	0.09
210	1.72	0.11	0.10	1.64	0.03	0.04	1.72	0.09	0.03	1.60	0.01	0.03	1.46	0.17	0.16	1.45	0.05	0.13
240	1.95	0.12	0.04	1.90	0.03	0.05	1.72	0.07	0.12	1.64	0.06	0.08	1.89	0.02	0.14	1.52	0.04	0.22
270	1.97	0.14	0.06	2.00	0.03	0.06	1.99	0.03	0.04	1.89	0.05	0.07	1.93	0.02	0.09	1.98	0.02	0.42

Table 5.35: Fault Index Variation with different locations and fault incidence angles for BG Fault

FIA	0			30			60			90			120			150		
	A	B	C	A	B	C	A	B	C	A	B	C	A	B	C	A	B	C
30	0.11	1.39	0.10	0.06	1.12	0.19	0.10	0.80	0.16	0.02	1.15	0.03	0.15	1.72	0.03	0.04	1.31	0.04
60	0.14	0.71	0.04	0.03	1.07	0.13	0.03	0.43	0.17	0.01	0.74	0.10	0.13	1.69	0.02	0.11	1.42	0.01
90	0.15	0.79	0.03	0.08	1.04	0.03	0.05	0.47	0.11	0.01	0.48	0.11	0.07	1.75	0.01	0.05	1.45	0.01
120	0.07	0.67	0.04	0.09	0.83	0.04	0.07	0.66	0.12	0.00	0.50	0.08	0.07	1.77	0.03	0.09	1.43	0.01
150	0.05	0.49	0.02	0.15	1.02	0.04	0.02	0.69	0.11	0.00	0.41	0.08	0.04	1.81	0.02	0.05	1.65	0.01
180	0.12	1.22	0.08	0.01	1.03	0.05	0.01	0.51	0.14	0.00	1.09	0.06	0.02	1.92	0.02	0.09	1.79	0.01
210	0.08	1.03	0.08	0.00	1.04	0.07	0.02	0.61	0.18	0.00	0.96	0.03	0.03	1.97	0.01	0.04	1.91	0.01
240	0.01	0.76	0.07	0.02	1.06	0.08	0.02	0.78	0.15	0.00	0.81	0.02	0.04	2.00	0.01	0.05	1.93	0.02
270	0.08	1.04	0.14	0.09	1.10	0.10	0.03	1.11	0.16	0.00	0.82	0.01	0.05	1.99	0.01	0.01	1.96	0.01

Table 5.36: Fault Index Variation with different locations and fault incidence angles for CG Fault

FIA	0			30			60			90			120			150		
Location	A	B	C	A	B	C	A	B	C	A	B	C	A	B	C	A	B	C
30	0.06	0.02	0.77	0.03	0.01	0.78	0.06	0.02	1.56	0.05	0.06	1.67	0.12	0.05	1.06	0.07	0.05	0.91
60	0.03	0.02	0.95	0.07	0.00	0.96	0.01	0.01	1.57	0.02	0.18	1.64	0.09	0.05	0.98	0.06	0.08	0.63
90	0.00	0.02	1.06	0.16	0.00	1.04	0.06	0.01	1.61	0.02	0.12	1.60	0.03	0.01	1.01	0.06	0.07	0.70
120	0.02	0.03	0.84	0.20	0.00	0.83	0.09	0.01	1.54	0.01	0.09	1.58	0.04	0.05	1.00	0.15	0.06	0.55
150	0.03	0.04	0.52	0.15	0.00	0.50	0.03	0.01	1.71	0.01	0.05	1.61	0.04	0.05	0.42	0.01	0.06	0.98
180	0.01	0.01	0.62	0.11	0.01	1.14	0.05	0.02	1.94	0.01	0.09	1.67	0.00	0.16	0.43	0.11	0.17	0.82
210	0.02	0.01	0.62	0.12	0.01	1.19	0.07	0.03	1.99	0.01	0.07	1.77	0.00	0.19	0.53	0.09	0.04	0.33
240	0.02	0.01	0.74	0.18	0.01	0.40	0.11	0.05	2.00	0.01	0.08	1.94	0.05	0.05	0.65	0.04	0.06	0.34
270	0.05	0.01	0.77	0.02	0.02	0.45	0.10	0.13	1.90	0.03	0.11	1.94	0.07	0.10	0.82	0.04	0.06	0.63

Table 5.37: Fault Index Variation with different locations and fault incidence angles for AB Fault

FIA	0			30			60			90			120			150		
Location	A	B	C	A	B	C	A	B	C	A	B	C	A	B	C	A	B	C
30	1.52	1.57	0.09	1.57	1.58	0.13	1.61	1.58	0.12	1.63	1.59	0.10	1.60	1.58	0.12	1.51	1.32	0.14
60	1.78	1.58	0.10	1.86	1.58	0.12	1.53	1.60	0.12	1.55	1.59	0.10	1.58	1.58	0.12	1.64	1.31	0.15
90	1.76	1.57	0.09	1.70	1.61	0.12	1.47	1.59	0.11	1.47	1.60	0.10	1.47	1.60	0.11	1.63	1.40	0.15
120	1.91	1.58	0.10	1.78	1.57	0.11	1.60	1.60	0.10	1.56	1.61	0.10	1.59	1.60	0.10	1.69	1.37	0.14
150	1.95	1.60	0.08	1.86	1.60	0.09	1.97	1.67	0.09	1.61	1.61	0.09	1.58	1.59	0.09	1.78	1.38	0.12
180	1.66	1.67	0.13	1.61	1.82	0.13	1.93	1.72	0.12	1.60	1.55	0.19	1.57	1.66	0.19	1.65	1.51	0.16
210	1.80	1.63	0.24	1.96	1.62	0.17	1.72	1.76	0.13	1.48	1.75	0.13	1.58	1.65	0.14	1.45	1.67	0.11
240	1.98	1.69	0.18	1.96	1.62	0.17	1.97	1.78	0.09	1.56	1.70	0.08	1.48	1.73	0.10	1.46	1.57	0.08
270	1.90	1.78	0.12	1.99	1.55	0.05	1.99	1.98	0.06	1.92	1.73	0.06	1.48	1.83	0.06	1.58	1.60	0.06

Table 5.38: Fault Index Variation with different locations and fault incidence angles for BC Fault

FIA	0			30			60			90			120			150		
Location	A	B	C	A	B	C	A	B	C	A	B	C	A	B	C	A	B	C
30	0.04	1.83	1.86	0.04	1.86	1.86	0.05	1.86	1.82	0.04	1.85	1.95	0.01	1.80	1.78	0.00	1.58	1.87
60	0.04	1.83	1.83	0.03	1.84	1.83	0.04	1.83	1.86	0.04	1.81	1.89	0.02	1.79	1.82	0.00	1.52	1.86
90	0.03	1.83	1.85	0.03	1.82	1.83	0.03	1.82	1.86	0.03	1.82	1.87	0.02	1.79	1.82	0.00	1.60	1.91
120	0.02	1.78	1.84	0.01	1.78	1.85	0.02	1.81	1.80	0.03	1.76	1.88	0.03	1.67	1.93	0.01	1.56	1.86
150	0.01	1.76	1.82	0.01	1.77	1.83	0.01	1.77	1.85	0.02	1.75	1.87	0.03	1.67	1.78	0.01	1.53	1.68
180	0.02	1.76	1.86	0.04	1.86	1.91	0.13	1.81	1.91	0.17	1.77	1.96	0.07	1.89	1.83	0.02	1.76	1.86
210	0.12	1.79	1.91	0.08	1.77	1.92	0.12	1.81	1.93	0.16	1.83	1.98	0.05	1.81	1.88	0.05	1.81	1.88
240	0.15	1.78	1.90	0.14	1.83	1.94	0.15	1.79	1.95	0.11	1.81	1.97	0.04	1.77	1.86	0.02	1.92	1.85
270	0.09	1.79	1.92	0.09	1.72	1.95	0.07	1.81	1.97	0.069	1.81	1.951	0.03	1.81	1.89	0.01	1.72	1.90

Table 5.39: Fault Index Variation with different locations and fault incidence angles for AC Fault

FIA	0			30			60			90			120			150		
	A	B	C	A	B	C	A	B	C	A	B	C	A	B	C	A	B	C
30	1.46	0.12	1.75	1.61	0.16	1.92	1.98	0.04	1.72	2.00	0.01	1.88	1.46	0.01	1.65	1.46	0.01	1.73
60	1.47	0.12	1.71	1.56	0.18	1.85	1.93	0.05	1.77	1.93	0.01	1.92	1.45	0.01	1.69	1.45	0.01	1.70
90	1.46	0.12	1.70	1.45	0.12	1.76	1.47	0.07	1.78	1.65	0.01	1.95	1.46	0.01	1.66	1.45	0.01	1.71
120	1.46	0.12	1.70	1.44	0.15	1.77	1.44	0.10	1.53	1.43	0.02	1.96	1.43	0.01	1.78	1.45	0.01	1.67
150	1.61	0.12	1.71	1.41	0.17	1.70	1.54	0.12	1.73	1.44	0.02	1.94	1.52	0.01	1.59	1.76	0.01	1.62
180	1.79	0.18	1.60	1.89	0.15	1.61	1.99	0.04	1.59	1.92	0.01	1.98	1.60	0.00	1.61	1.90	0.01	1.59
210	1.95	0.13	1.59	1.99	0.09	1.60	1.97	0.03	1.60	1.91	0.01	1.94	1.46	0.00	1.58	1.27	0.01	1.58
240	1.98	0.08	1.59	1.98	0.07	1.58	1.94	0.02	1.57	1.41	0.01	1.88	1.95	0.01	1.57	1.35	0.01	1.57
270	1.84	0.05	1.57	1.93	0.05	1.57	1.98	0.02	1.57	1.76	0.01	1.77	2.00	0.01	1.56	1.92	0.02	1.58

Table 5.40: Fault Index Variation with different locations and fault incidence angles for ABG Fault

FIA	0			30			60			90			120			150		
	A	B	C	A	B	C	A	B	C	A	B	C	A	B	C	A	B	C
30	1.54	1.63	0.03	1.51	1.65	0.17	1.82	1.66	0.15	1.77	1.66	0.03	1.79	1.64	0.03	1.68	1.38	0.02
60	1.59	1.64	0.12	1.68	1.64	0.04	2.00	1.65	0.07	1.89	1.65	0.15	1.91	1.62	0.07	1.77	1.35	0.03
90	1.81	1.63	0.13	1.77	1.66	0.13	1.87	1.64	0.15	1.93	1.66	0.10	1.93	1.62	0.09	1.92	1.45	0.06
120	1.89	1.63	0.18	1.80	1.61	0.12	1.89	1.65	0.16	1.93	1.67	0.11	1.95	1.63	0.10	1.93	1.44	0.11
150	1.79	1.64	0.12	1.84	1.64	0.12	1.89	1.69	0.13	1.93	1.67	0.12	1.96	1.66	0.10	1.88	1.45	0.09
180	2.00	1.77	0.14	1.75	1.82	0.14	1.66	1.74	0.13	1.48	1.59	0.16	1.49	1.69	0.08	1.58	1.55	0.10
210	1.73	1.67	0.21	2.00	1.62	0.14	1.58	1.77	0.11	1.39	1.77	0.17	1.54	1.69	0.07	1.38	1.71	0.11
240	1.99	1.72	0.19	1.98	1.84	0.16	1.99	1.75	0.18	1.84	1.76	0.12	1.46	1.73	0.12	1.49	1.63	0.14
270	2.00	1.77	0.14	1.99	1.54	0.13	1.95	1.95	0.13	2.00	1.72	0.14	1.58	1.85	0.13	1.70	1.57	0.08

Table 5.41: Fault Index Variation with different locations and fault incidence angles for BCG Fault

FIA	0			30			60			90			120			150		
	A	B	C	A	B	C	A	B	C	A	B	C	A	B	C	A	B	C
30	0.11	1.02	0.22	0.04	1.18	1.24	0.14	0.68	1.77	0.00	0.90	1.84	0.01	1.68	0.78	0.08	1.45	0.97
60	0.06	1.56	1.14	0.10	1.15	1.23	0.07	0.65	1.78	0.00	1.04	1.88	0.01	1.71	0.90	0.04	1.44	0.95
90	0.06	1.54	1.12	0.17	0.81	1.20	0.13	0.66	1.78	0.00	0.90	1.87	0.02	1.68	0.88	0.03	1.51	0.82
120	0.04	1.40	1.26	0.10	1.11	1.25	0.12	0.66	1.76	0.00	0.82	1.89	0.02	1.63	1.12	0.09	1.49	0.74
150	0.03	1.36	1.24	0.16	0.80	1.20	0.03	0.81	1.78	0.01	0.71	1.90	0.02	1.65	1.50	0.20	1.55	0.39
180	0.06	1.05	1.12	0.09	1.14	1.17	0.02	0.79	1.78	0.00	0.83	1.97	0.01	1.89	1.02	0.07	1.73	0.33
210	0.04	1.05	1.16	0.09	1.10	1.19	0.04	1.02	1.80	0.00	0.79	1.95	0.01	1.80	1.02	0.13	1.90	0.38
240	0.01	1.00	1.18	0.17	1.09	1.20	0.07	1.06	1.76	0.00	0.73	1.92	0.01	1.77	0.87	0.11	1.71	0.83
270	0.07	0.77	1.18	0.10	1.10	1.18	0.06	1.01	1.70	0.02	0.73	1.86	0.01	1.80	0.91	0.02	1.68	1.31

Table 5.42 Fault Index Variation with different locations and fault incidence angles for ACG Fault

FIA	0			30			60			90			120			150		
	A	B	C	A	B	C	A	B	C	A	B	C	A	B	C	A	B	C
30	1.92	0.03	1.03	1.83	0.03	1.04	0.60	0.02	1.63	0.85	0.19	1.82	1.24	0.07	1.08	1.38	0.07	0.42
60	1.55	0.03	0.99	1.94	0.02	1.02	0.53	0.01	1.61	0.62	0.06	1.90	1.26	0.05	0.99	1.38	0.06	0.54
90	1.47	0.02	1.02	1.97	0.01	1.05	0.48	0.01	1.59	0.43	0.06	1.92	1.24	0.04	0.99	1.37	0.16	0.80
120	1.51	0.09	1.02	2.00	0.01	1.04	0.43	0.01	1.63	0.56	0.04	1.93	1.24	0.03	1.14	1.39	0.09	1.03
150	1.50	0.07	1.03	1.98	0.01	1.00	0.42	0.01	1.55	0.76	0.03	1.91	0.84	0.02	1.37	1.34	0.09	0.86
180	1.63	0.04	1.00	1.95	0.00	1.04	0.40	0.01	1.52	0.52	0.03	1.97	1.22	0.14	0.97	1.24	0.19	1.00
210	1.53	0.04	0.74	1.87	0.00	0.91	0.38	0.01	1.70	0.35	0.02	1.93	1.23	0.16	1.00	1.26	0.14	0.90
240	1.51	0.02	0.84	1.90	0.00	0.70	0.35	0.01	1.62	0.33	0.03	1.88	0.99	0.17	0.96	1.38	0.14	0.88
270	1.51	0.01	1.04	1.89	0.00	0.69	0.33	0.01	1.53	0.71	0.04	1.77	0.52	0.11	0.90	0.97	0.16	1.00

Table 5.43 Fault Index Variation with different locations and fault incidence angles for ABCG Fault

FIA	0			30			60			90			120			150		
	A	B	C	A	B	C	A	B	C	A	B	C	A	B	C	A	B	C
30	1.91	1.62	1.68	1.83	1.68	1.81	1.95	1.67	1.69	1.33	1.68	1.87	1.30	1.64	1.59	1.40	1.43	1.73
60	1.93	1.66	1.69	1.80	1.67	1.76	1.90	1.67	1.75	1.52	1.67	1.89	1.32	1.65	1.69	1.32	1.46	1.69
90	1.96	1.67	1.68	1.83	1.68	1.74	1.99	1.66	1.76	1.50	1.68	1.87	1.36	1.63	1.64	1.41	1.59	1.76
120	1.96	1.65	1.66	1.83	1.62	1.75	1.99	1.66	1.61	1.46	1.66	1.87	1.39	1.61	1.84	1.38	1.59	1.71
150	1.94	1.80	1.69	1.84	1.53	1.70	1.84	1.53	1.70	1.55	1.72	1.72	1.46	1.77	1.64	1.78	1.50	1.68
180	2.00	1.72	1.69	1.91	1.80	1.70	1.68	1.72	1.70	1.38	1.71	1.94	1.49	1.77	1.67	1.28	1.57	1.68
210	1.99	1.69	1.71	1.73	1.66	1.70	1.98	1.73	1.68	1.70	1.71	1.89	1.33	1.71	1.68	1.35	1.74	1.68
240	1.99	1.70	1.70	1.93	1.79	1.70	1.99	1.72	1.69	1.33	1.72	1.84	1.84	1.69	1.66	1.34	1.58	1.68
270	1.93	1.77	1.69	1.81	1.59	1.70	2.00	1.82	1.71	1.43	1.69	1.76	1.37	1.74	1.67	1.62	1.55	1.68

(c) Variation of Fault Impedance

Faults with high impedances are difficult to detect due to low level of post-fault currents owing to low sensitivity of the relay. The sensitivity of the proposed protection scheme has been established by selecting the fault impedances from 0-100Ω under this case study. Figure 5.33 illustrates the fault index variation of all the three-phases for different types of faults, for a fault impedance of 15Ω. Figure 5.33(a) depicts that the fault index of phase-A is higher than the threshold and for other phases it is less than the threshold at all the locations hence it is detected as AG fault. From Figures 5.33(b) and 5.33(c), it is observed that for phase-A and B, value of fault indexes is more than the threshold and not for phase-C, and hence the faults are detected as AB and ABG respectively. It is evident from Figure 5.33(d) that the index value of all the three phases is more than the threshold; hence it is detected as ABCG fault.

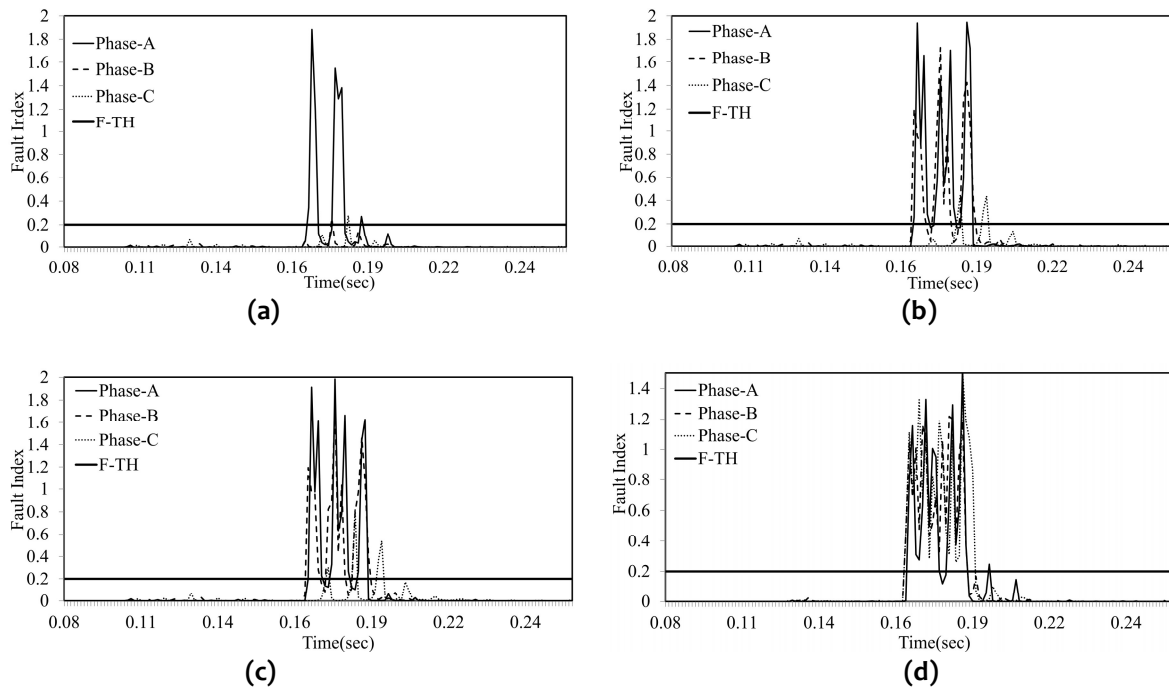


Figure 5.33: Fault Index Variation for high impedance faults: (a) AG Fault, (b) AB Fault, (c) ABG Fault, (d) ABCG Fault

(d) Effect of UPFC Location

The location of UPFC affects the magnitude and transients of bus-currents. Hence, the performance of the proposed algorithm is verified by changing the UPFC location to receiving end (Bus-2). Figures 5.34(a-d) illustrate the variation of three-phase fault index for AG, AB, ABG and ABCG faults respectively. From these figures, it can be observed that the fault index of faulty phases alone, exceed the threshold value. Hence, it is established that the location of UPFC does not affect the performance of the proposed algorithm.

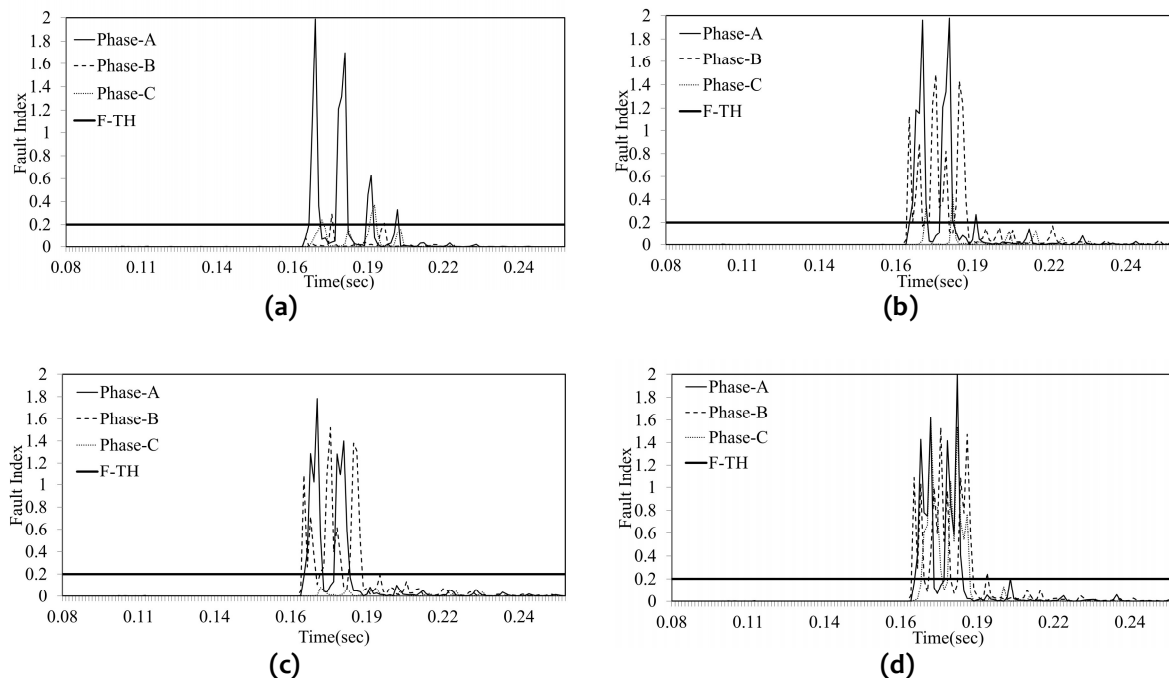


Figure 5.34: Fault Index Variation for UPFC installed at bus-2: (a) AG Fault, (b) AB Fault, (c) ABG Fault, (d) ABCG Fault

(e) Performance of Noisy Environment

The current signals are contaminated with noise to prove the robustness of the proposed scheme to detect and classify the faults in the noisy environment. For this purpose the levels of SNRs considered, is 40dB-10dB. Figure 5.35 depicts variation of three-phase fault index for different types of faults, with 10dB white Gaussian noise. Figure 5.35(a) depicts variation of fault index for AG fault. The fault index of phase-A is greater than the threshold and that of other phases is less than the threshold, thus illustrating AG fault. Figure 5.35(b) and 5.35(c) illustrate that for phase-A and phase-B, fault index is greater than the threshold and not for phase-C, and hence the fault is detected as AB and ABG fault. Figure 5.35(d) shows that for all the three phases, fault index is greater than the threshold. Hence it is detected as ABCG fault. Thus, it is proved that the proposed algorithm can detect and classify the faults even in the noisy environment.

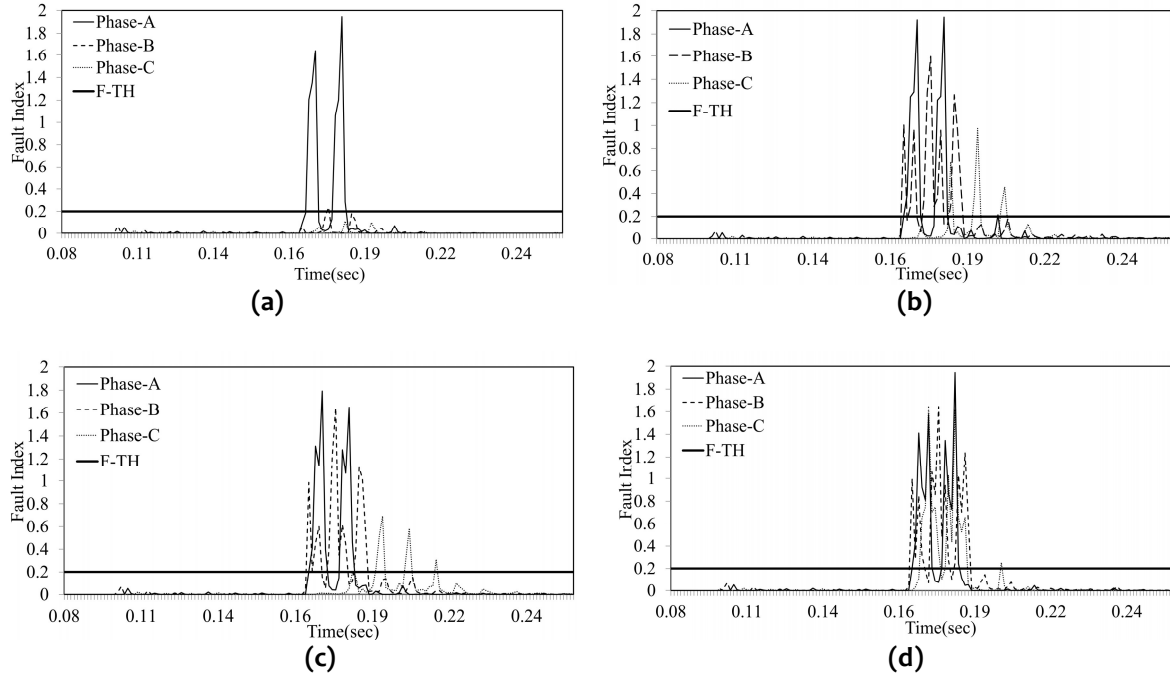


Figure 5.35: Fault Index variation for Noisy environment: (a) AG Fault, (b) AB Fault, (c) ABG Fault, (d) ABCG Fault

(f) Effect of Loading

Switching of loads also causes transients in current signals which may affect the performance of proposed protection algorithm, which works on the on basis of current signals. Hence, the performance of the proposed algorithm has been evaluated for 10% and 20 % of load changes. The highest fault indexes associated with the load switching is found to be 0.06 which is very low as compared to threshold (0.2) value. Thus, it is evident that the proposed algorithm has not been affected by load switching.

(g) Effect of Power-Flow Direction

To consider the effect of power-flow direction in the proposed algorithm, it has been tested on reverse power flow condition. Since the proposed scheme is making use of data from both the buses, the obtained results corresponding to reverse power-flow are found to be same as in case of original power flow.

(h) Effect of Sampling Frequency

The algorithm has been tested with sampling frequency of 0.96 kHz, 1.92 kHz, 3.84 kHz and 7.68 kHz; it has been observed that increase in frequency has no considerable improvement in terms of accuracy and speed of proposed protection scheme. However the reduction in sampling frequency increases the detection time.

5.5.4 Location of Fault

Estimation of fault location has been carried out, followed by fault detection and classification, using Artificial Neural Network. A multi-layer feed-forward neural network, whose structure is shown in Figure 5.35, is used to locate the fault. The details related to structure of ANN are presented in Table 5.44.

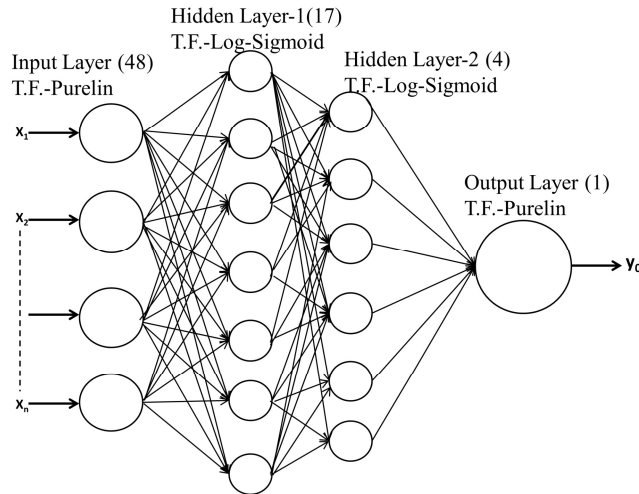


Figure 5.35: ANN Structure

Table 5.44: Structure of ANN

S. No.	Name of Layers	No. of Neurons	Transfer Function
1	Input Layer	48	Purelin
2	Hidden-Layer-1	17	Log-Sigmoid
3	Hidden- Layer-2	4	Log-Sigmoid
4	Output Layer	1	Purelin

The input to neural network is 4-approximate coefficients, of each phase voltage and current signal, obtained over a quarter cycle, from both the ends of the line. Thus, the total number of inputs is $[2(\text{buses}) * \{3(\text{phase voltage}) + 3(\text{phase current})\}] * 4$ coefficients.

The output of the ANN will be fault location (in kms) from bus-1. The training of proposed ANN has been carried out by feeding 48 approximate coefficients of post-fault three-phase voltage and current signals, obtained over a quarter cycle. The trained ANN has been tested for its performance with the data obtained by data obtained from simulating all the types of faults at new locations. The percentage error (\mathcal{E}) in fault location is calculated as:-

$$\%Error = \frac{|NNDistance - ActualDistance|}{L} * 100$$

Table 5.45 demonstrates the accuracy using proposed ANN. From this, it can be observed that the maximum and average error, in locating the faults, is 2.60% and 0.72% respectively.

Table 5.45: Estimation of Fault Location

S.No	Fault-type	Actual Location	ANN Location	% Error
1	Phase-A to G	42	37.86	1.38
2	Phase-A to G	101	100.54	0.15
3	Phase-A to G	174	171.26	0.91
4	Phase-A to G	231	230.17	0.28
5	Phase-B to G	42	46.63	1.54
6	Phase-B to G	101	101.07	0.02
7	Phase-B to G	174	175.16	0.39
8	Phase-B to G	231	231.20	0.07
9	Phase-C to G	42	40.73	0.42
10	Phase-C to G	101	101.61	0.20
11	Phase-C to G	174	174.12	0.04
12	Phase-C to G	231	229.42	0.53
13	Phase-A to B	42	40.76	0.41
14	Phase-A to B	101	101.72	0.24
15	Phase-A to B	174	170.47	1.18
16	Phase-A to B	231	230.24	0.25
17	Phase-B to C	42	42.28	0.09
18	Phase-B to C	101	98.83	0.72
19	Phase-B to C	174	170.95	1.02
20	Phase-B to C	231	228.74	0.75
21	Phase-A to C	42	39.62	0.79
22	Phase-A to C	101	100.93	0.02
23	Phase-A to C	174	174.25	0.08
24	Phase-A to C	231	227.03	1.32
25	Phases-AB to G	42	39.29	0.90
26	Phases-AB to G	101	101.61	0.20
27	Phases-AB to G	174	176	0.67
28	Phases-AB to G	231	230.52	0.16
29	Phases-BC to G	42	39.23	0.92
30	Phases-BC to G	101	101.16	0.05
31	Phases-BC to G	174	176.57	0.86
32	Phases-BC to G	231	227.95	1.02
33	Phases-AC to G	42	49.80	2.60
34	Phases-AC to G	101	100.83	0.06
35	Phases-AC to G	174	168.61	1.80
36	Phases-AC to G	231	227.85	1.05
37	Phases-ABC to G	42	45.13	1.04
38	Phases-ABC to G	101	102.35	0.45
39	Phases-ABC to G	174	176.35	0.78
40	Phases-ABC to G	231	231.75	0.25

5.5.5 Performance in Absence of UPFC

In this section, efforts have been made to prove the ability of algorithm to detect and classify the faults, even in the absence of UPFC (due to maintenance or outage). For this purpose, UPFC has been disconnected from the transmission line and various types of faults have been simulated. Table-4 compares the performance of proposed protection scheme with and without presence of UPFC. From this table, it can be observed that the fault indexes of faulty phases remains higher than the threshold, both in presence and absence of UPFC. The performance of proposed ANN has been evaluated in absence of UPFC for all the types of faults and results are shown in Tables 5.46-5.47. Thus, it is evident that the proposed algorithm is not affected by presence or absence of UPFC.

Table 5.46: Performance Comparison

S. No.	Fault Type	Phase-A		Phase-B		Phase-C	
		Without UPFC	With UPFC	Without UPFC	With UPFC	Without UPFC	With UPFC
1	AG	1.18	1.20	0.05	0.06	0.01	0.01
2	BG	0.06	0.09	1.38	1.14	0.01	0.01
3	CG	0.10	0.11	0.01	0.01	0.90	0.95
4	AB	1.37	1.25	0.98	1.00	0.01	0.01
5	BC	0.01	0.01	1.43	1.38	0.96	0.95
6	AC	1.42	1.49	0.01	0.01	0.74	0.76
7	ABG	1.28	1.31	1.02	0.98	0.01	0.01
8	BCG	0.04	0.05	1.40	1.10	0.68	0.78
9	ACG	1.50	1.46	0.03	0.04	0.73	0.66
10	ABC	1.36	1.44	0.86	0.99	1.09	1.07

Table 5.47: Fault Location for system without UPFC

S.No	Fault-type	Actual Location	ANN Location	% Error
1	AG	35	36.84	0.61
2	BG	84	81.52	0.82
3	CG	105	105.55	0.18
4	AB	75	78.90	1.30
5	BC	150	149.61	0.39
6	AC	268	265.32	0.89
7	ABG	69	70.00	0.33
8	BCG	187	185.98	0.34
9	ACG	250	253.12	1.04
10	ABCG	53	53.69	0.23

5.6 CONCLUSION

A wavelet-alienation based protection scheme has been proposed to detect, classify and locate the faults on transmission line, operating with various FACTS devices. Approximate decomposition of current signals, obtained over a quarter cycle, are compared in terms of alienation coefficients to detect and classify faults. Estimation of fault location has been carried out by ANN, which is fed from approximate coefficients of three-phase voltage and current signals. The average error in fault location is found to be 0.87%. Thus, the proposed algorithm was found to be successful in detection and classification of faults with variations in fault

location, incidence angle and fault impedance, noise contamination, power flow direction and load switching. It has also been proved that type of FACTS device used, TCSC, STATCOM or UPFC and the location of FACTS device, has no effect on proposed algorithm.

